WATER QUALITY IN THE LEON CREEK WATERSHED RECHARGE ZONE AS A FUNCTION OF URBAN DEVELOPMENT, AND COMMUNITY EDUCATION OF THE THREATS AND CONSERVATION OF THE EDWARD'S AQUIFER

A City of San Antonio, Edwards Aquifer Protection Venue program funded project

FINAL REPORT PREPARED FOR:

City of San Antonio
Parks and Recreation Department
Edwards Aquifer Protection Program

and

San Antonio River Authority





BRIAN G. LAUB MELISSA GARCIA ANDREW PARDOE LANI MAY FELIPE VILLANUEVA

The University of Texas at San Antonio San Antonio, Texas





June 30, 2024

EXECUTIVE SUMMARY

Expanding urban development in San Antonio and surrounding communities poses a threat to the region's aquatic resources, including the Edwards Aquifer. Urban development impacts water resources by increasing stormwater runoff and pollutant delivery to downstream waters. There is growing interest in using green infrastructure, or low impact development (LID) facilities, to help manage stormwater runoff and pollutant loading from newly constructed and existing urban areas. However, there exists uncertainty as to how urban development impacts water quality in stormwater runoff in the recharge zone area of the Edwards Aquifer and as to the feasibility and benefits of implementing green stormwater infrastructure in the region.

In 2018, funding was obtained through the City of San Antonio's Edwards Aquifer Protection Venue Program to...

Introduction

- a. Urbanization causing problems
- **b.** Management needed
- c. To inform management need local understanding of impacts
 - i. May be less of an issue in SA where soils somewhat thin anyway
- d. Green infrastructure can be used for management
 - i. But need to know if effective, design considerations for optimal performance
- **e.** Something about how education is also important, having demonstration BMPs can help with education
- f. Objectives
 - i. Understand urban development impacts on stormwater runoff, channel morphology, and water quality
 - **ii.** Test effectiveness of green infrastructure hydrologically and water quality-wise
 - 1. Bioretention basins relative to a natural system
 - iii. Provide a facility and programs for education
 - 1. Demonstration facilities including green roof and cistern

Objective 1 – Water Quality, Hydrology, and Riparian Vegetation as a Function of Urban Development

Project Implementation

Site Locations

A total of 12 sites were monitored for Objective 1 (Figure 1.1, Table 1.1). All sites except four were located in the Leon Creek watershed and were chosen to sample a gradient of watershed urbanization from highly urban to completely forested. Ten sites were monitored for flow and water quality over the duration of the project, and six of these sites were also surveyed for channel morphology and riparian vegetation. Two of the ten sites monitored for flow and water quality (Government Canyon 1 and 2) did not have any flow events occur over a monitoring period of approximately one year. Thus, two sites were added (San Geronimo Front and Back) to replace the original sites. Two additional sites (Salado Creek and Leon Creek mainstem) were sampled only for channel morphology and riparian vegetation.

Land use data for each site were obtained from the EPA's StreamCat Dataset where possible, which links National Land Cover Database (NLCD) information to individual stream segments and catchments of the National Hydrography Dataset (Hill et al. 2016). For some sites with small watersheds, including LaCantera (others?), StreamCat data were not available. For these sites, land use data was obtained through a GIS analysis in which watersheds were delineated and used to clip the NLCD land use data layer. Equivalent data to StreamCat data was obtained using the clipped land

use shapefiles. Land use metrics from the 2019 NLCD were used in this study and included percent impervious cover, percent low-, medium- and high-intensity urban cover, percent forest cover, percent shrubland cover, and percent agricultural cover in the watershed and catchment of each site, as these were the most common land use types in the watershed. Agricultural cover is defined as the sum of cropland and hay land.

Table 1.1. Study sites used for Objective 1, site characteristics, and information on what each site was used for and date ranges active sampling occurred

Site	Impervious cover (%)	Watershed Area (km²)	Data Collected	Dates Active
Government	1.0	37.9	, ,	
Canyon 1			Water Quality	
			Riparian Veg	
Government	0.0	2.3	Hydrology	
Canyon 2			Water Quality	
			Riparian Veg	
Madla	0.3	15.3	Hydrology	
			Water Quality	
Mayberry	0.6	10.5	Hydrology	
			Water Quality	
San Geronimo	2.1	12.3	Hydrology	
Front			Water Quality	
San Geronimo	0.1	21.3	Hydrology	
Back			Water Quality	
French	41.2	19.1	Hydrology	
			Water Quality	
			Riparian Veg	
Huesta	19.4	6.1	Hydrology	
			Water Quality	
			Riparian Veg	
La Cantera	45.2	2.7	Hydrology	
			Water Quality	
			Riparian Veg	
Maverick	18.1	17.9	Hydrology	
			Water Quality	
			Riparian Veg	
Leon	18.1	112.3	Riparian Veg	N/A
Salado	12.1	91.3	Riparian Veg	N/A

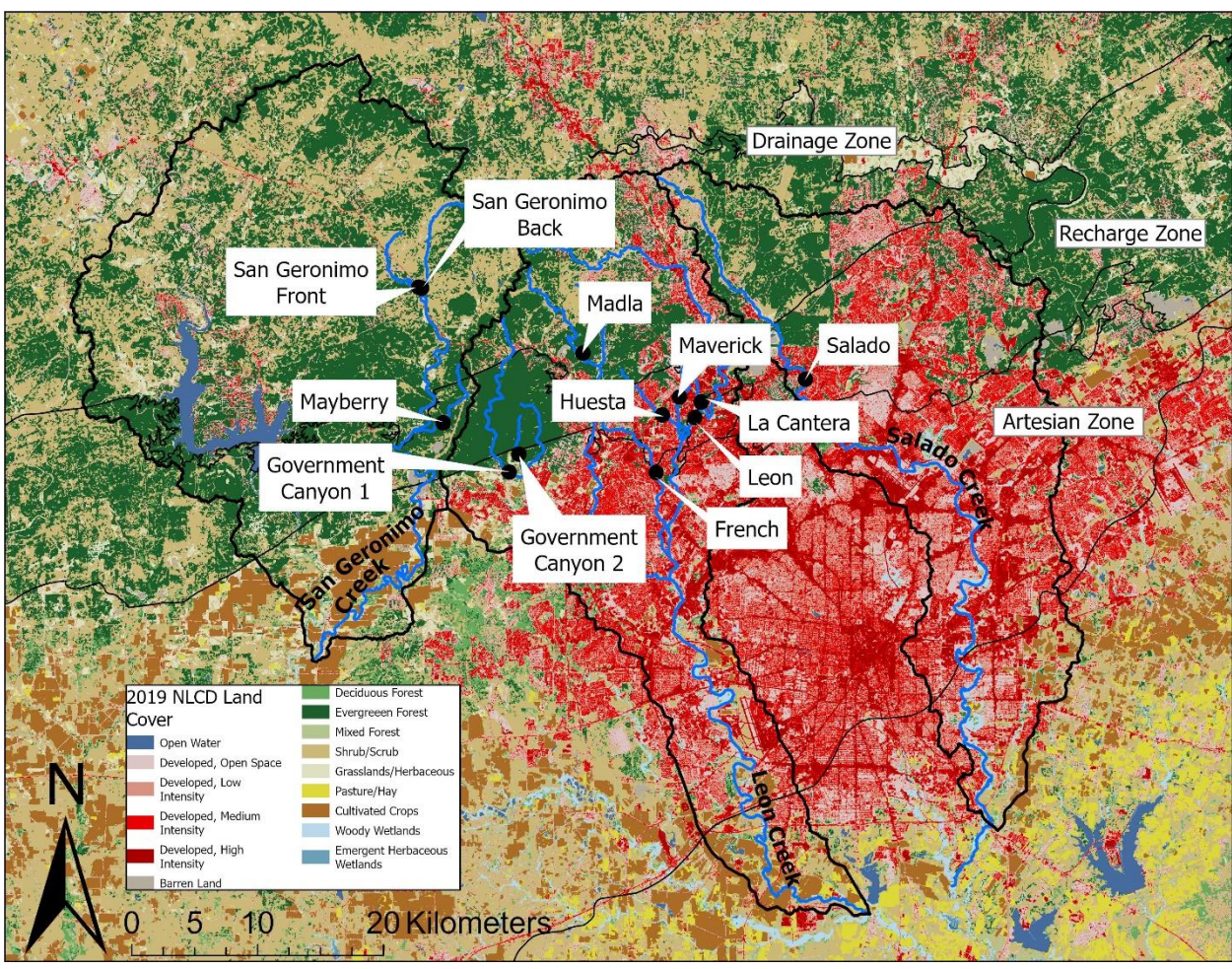


Figure 1.1. Map showing the locations of study sites within the San Geronimo, Leon, and Salado Creek watersheds and within the different zones of the Edwards Aquifer. Background map shows 2019 land cover from the National Land Cover Database (NLCD).

Water quality and Hydrology Sampling

Flow meters and automatic water samplers

Flow-paced sampling of multiple flushes

Water taken back to lab for processing

In-situ temperature monitors

Riparian vegetation Sampling

Following sampling protocols established by Scott & Reynolds (2007), the overall goal of channel surveys was to measure diversity and community composition of the riparian vegetation on multiple geomorphic surfaces at each site, with vegetation measured by canopy coverage, basal area, and stem density. The length of each channel survey was 10 times the average floodplain width, but with a minimum and

maximum length of 300 & 800 meters, respectively. Floodplain width was defined as starting from the edge of the active channel to the tree line of the riparian terrace (Figure 1.2). Average width was calculated from measurements of the floodplain width at five transects.

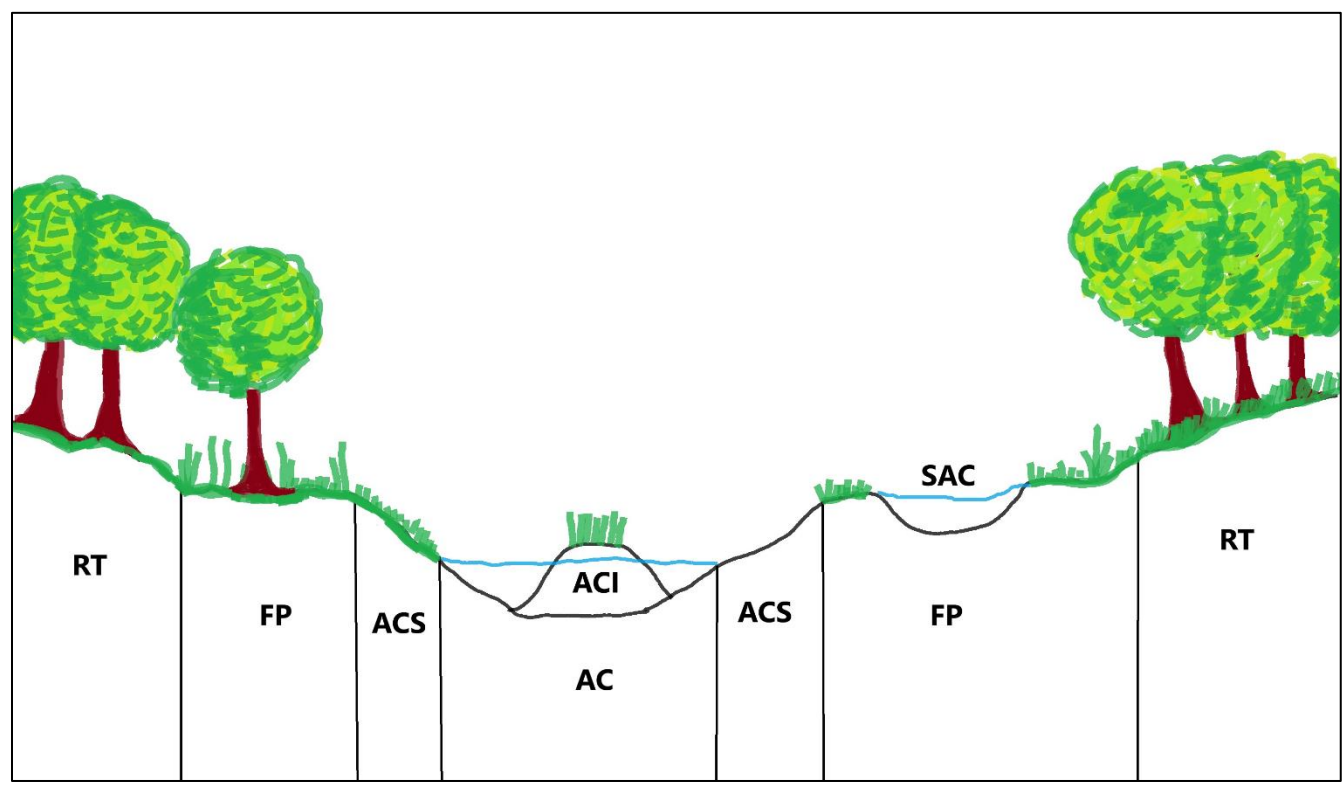


Figure 1.2. Illustration defining the location of geomorphic surfaces within a creek or stream system. It should be noted that not all geomorphic features were expected to occur, with AC = active channel, ACI = active channel island, ACS = active channel shelf, FP = floodplain, SAC = secondary active channel RT = riparian terrace. Drawing credit: Leslie Vega-Garcia

Transect Layout

At each stream eleven survey transects plotted orthogonal to the down-valley axis of the floodplain were established and numbered in ascending order, starting downstream and proceeding upstream. Transects were spaced evenly apart along the channel thalweg by dividing the overall survey length by ten and had a minimum spacing of 30 meters and maximum of 80 meters. Transects crossed the width of the floodplain into the riparian terrace on both sides of the channel and GPS coordinates of the endpoints of each transect were recorded for position reference and future use.

Data collection: Line Intercept

Using a line intercept method, we surveyed canopy coverage every meter along each transect, where woody species and shrubs were identified to species and

categorized by canopy height and as native or non-native. Additionally, geomorphic surface type was recorded at each measurement point and consisted of the active channel (AC; lowest elevation, marked by substrate ranging from sand to boulder), secondary active channel (SAC; found in the floodplain, with a lower elevation profile than its surroundings, marked by substrate ranging from sand to boulder as found in the active channel, and showed signs of water flow), active channel shelf (ACS; angled slope found between the active channel and floodplain, and ranged from a gentle to incised angles, with similar substrate to the active channel), floodplain (FP; large flat open space above the active channel with gaps in the canopy, typically had grasses and small poles, with finer substrate such as sand), stream islands (ISL; located in the active channel having a slighter higher elevation profile, and could be completely submerged during high volume flow events. It also had a similar vegetation and substrate profile found in the floodplain) and riparian terrace (RT; highest elevation, marked off by a tree line of veteran age, low abundance of grasses, and an enclosed canopy; Figure 2).

In addition, a topographic survey was conducted using an auto-level along each transect to determine the cross-section elevation profile of each transect, which assisted in properly classifying geomorphic surfaces based on slope breaks and relative elevation.

Quadrat Sampling

Using quadrat sampling, we gathered data on stem density and basal area (diameter at breast height -DBH) to understand the abundance of individual species. One quadrat was surveyed on each geomorphic surface type along each transect, with center point locations of quadrats on identified geomorphic surfaces selected randomly from the total length of transect crossing each geomorphic surface type (Figure 1.3). Each quadrat extended 2.5 m upstream and downstream from the transect line and 2 meters along the transect, such that each quadrat was 2 meters wide x 5 meters long. Stem density was calculated by counting the individual stems of each woody species in each quadrat and dividing by the quadrat area (10 m²). Whereas the basal area was calculated by summing the DBH of all individual stems for each woody species. And if more than one stem shared a common trunk, we recorded each as being part of the same individual and aggregated the DBH (Porter et al., 2001, p. 135). In cases where a stem was located on the border of the quadrat, we followed Scott & Reynolds (2007) methods stating that at least 50 percent of a stem must be in the quadrant to be counted. Additionally, total area surveyed (m²), basal area (cm²), basal area per meter surveyed (cm²/m²), total stems, and stems per meter (stem/m²) were computed.

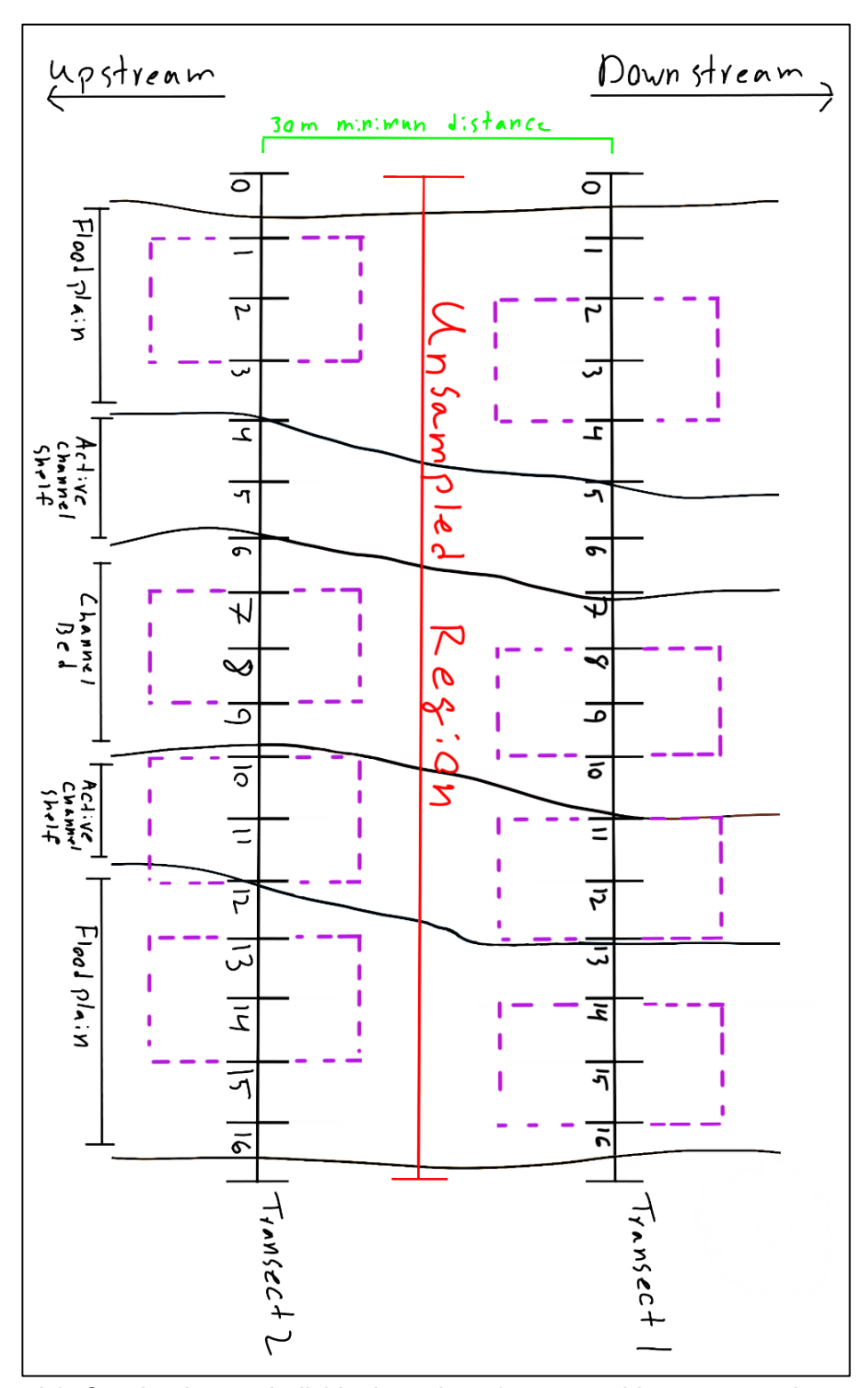


Figure 1.3. Quadrat layout. Individual quadrats 2 meters wide x 5 meters long extended outwards from each side of the transect line to capture elevation surfaces. Additionally, in consideration of whether a species was inside or outside of the quadrat the following rule was followed: if a stem is more than 50 percent outside of the quadrat, it was not included

Species Identification

Woody species were identified in the field using the following field manuals: Seek (iNaturalist, Version 2.15.2) and Trees, Shrubs, and Vines of the Texas Hill Country: A Field Guide (Jan Wrede, 2010). If a plant was difficult to identify, we took photographs and a sample for later identification and marked the datasheet with a question mark.

Data & Statistical Analysis

Riparian community diversity and trait calculations

We calculated Shannon-Weiner's Diversity Index and richness for each surveyed site using canopy cover, which was standardized by relative abundance. We further categorized riparian species as native or exotic, drought or non-drought tolerant, having low, medium, or high-water use, and having low, medium, high, or very high heat tolerance, and calculated canopy cover, basal area, and stem density of the different categories at the stream level for use in linear regression modeling.

Drought tolerance, heat tolerance, and water use were identified for each species by using the United States Department of Agriculture Plants Database (USDA, 2019). Native Plants Database, Lady Bird Johnson Wildflower Center: The University of Texas at Austin, Texas Native Shrubs: Texas A&M AgriLife Extension, Trees of Texas: Texas A&M Forest Service, Trees, Shrubs, and Vines of the Texas Hill Country: A Field Guide (Jan Wrede, 2010), and were assigned a numerical value (trait value) in order to run environmental fitting (Table 1.2).

Riparian community ordination

In order to visualize the dissimilarity of vegetation communities between the sites and between geomorphic surfaces, NMDS was run on composition of woody species for the entire site and on composition of woody species for each geomorphic surface type within sites. The analysis at the site level was done to help answer the question of whether sites differed in riparian community composition and trait abundances across a gradient of urbanization and flow regimes. The analysis at the geomorphic surface level was done to determine whether riparian communities grouped by geomorphic surface, regardless of site location. Separate NMDS models were run at the site level using each of the measures of riparian communities: canopy cover, basal area, and stem density, all standardized by relative abundance. Analysis at the geomorphic surface level only used relative abundance of canopy cover. For analysis on relative abundance of canopy cover at both the site and geomorphic surface level, the following conditions were used: Bray-Curtis dissimilarity, Wisconsin Double Standardization and square root transformation. Whereas relative abundance of basal area and stem density used: Bray-Curtis dissimilarity. All NMDS analyses were conducted in R using the vegan package (R Core Team, Oksanen et al. 2021)

Table 1.2. Assigned numerical values for woody species attributes

	Drought Tolerance						
1	Low						
2	Medium						
3	Medium High						
4	High						
5	Very High						
	Heat Tolerance						
1	Low						
2	Medium						
3	Medium High						
4	High						
5	Very High						
	Water Use						
1	Low						
2	Low Medium						
3	Medium						
4	High						
5	Low Medium High						
6	Low High						

Environmental Effects on Riparian Communities

Environmental fitting of land use, flow metrics, and woody species traits were used as explanatory variables in order to understand how sites grouped across an urbanization gradient. Using the numerical values assigned to woody species traits, a species by trait matrix was created, and then converted into a matrix of trait values per site level by multiplying the site by species matrix with the species by trait matrix, with the species relative abundance data of the canopy cover, basal area, and stem density. We fitted this new site by trait matrix to the NMDS of community composition to better understand whether sites had different trait compositions and whether trait compositions varied along a gradient of urbanization as expected. A matrix of land use and flow metric data for each site was also fitted to the NMDS of community composition to better understand how land use and flow varies and plots along the gradient of site dissimilarity determined by community composition. Fitting of land use, flow, and trait variables to the NMDS models was performed in R using the envfit function in the vegan package (R Core Team, Oksanen et al. 2021).

Effects of Impervious Cover on Hydrology and Riparian Vegetation

To determine if impervious cover was impacting flow metrics at each site, linear regression was used to test for a significant relationship between watershed impervious cover and both number of flood events per year and average period between floods. To determine if impervious cover was impacting riparian community diversity, linear regression was used to test whether there was a significant relationship between watershed percent impervious cover and species richness and Shannon diversity, where these values represented the overall site and were calculated from canopy cover only. Linear regression was also used to determine whether impervious cover was impacting species traits of the riparian community at the site level. The species traits tested were the following: drought tolerance, heat tolerance, water use, and native versus exotic. As an example, for drought tolerance, we ran a linear regression testing for a significant relationship between watershed impervious cover and relative abundance of all species classified as drought tolerant at a site. Species traits were also analyzed per site level and were calculated for all three measures of riparian communities (canopy cover, basal area, stem density). For this testing, we used relative abundances, assumed the data to be linear and had no extreme outliers, and used the linear modeling (lm) function in R (R Core Team).

Results

Number of events sampled and dates at each site

Ranges of hydrologic parameters such as number of events and range of peakflows etc.

Ranges of first flushes, event means, loads at each site

Statistical results of whether impervious cover influenced hydrologic metrics, first flush, event means, loads, channel morph and riparian veg

Riparian Vegetation

Across all eight locations sampled for riparian vegetation, a total of 43 species of shrub and trees were identified. Forty-one of these species were found in both the line transect and quadrat data collection. The remaining 2 species were only found in the quadrat surveys (Crataegus texana at Salado, and an unidentified species at Leon). Non-natives were uncommon across all sites regardless of urban development. Of the 43 species, 5 were non-native and composed 11.6% of the species count, whereas the remaining 38 species were native and composed 88.4% of the species count. Nonnatives represented 1.54% of the total canopy composition across all sites and had a total of 67 stems and total basal area of 122.24 cm². In comparison, native species represented 98.46% of the total canopy composition across all sites and had a total stem count of 8,112 and a total basal area of 13,801.21 cm². Diversity measured by canopy cover ranged from 1.11 to 2.18 with the lowest values at LaCantera and the highest values at Leon. Similarly, species richness ranged from 8 to 24 with LaCantera having the lowest values and Leon with the highest values (Table 3). Basal area ranged from 1.80 cm²/m² to 7.32 cm²/m² with the lowest value at French and Government Canyon 2 having the highest (Table 1.3). Stem density ranged from 0.50 stems/m² to 3.31 stems/m² with the lowest value at Leon and the highest at Government Canyon 2 (Table 1.3). Drought tolerant species were abundant at all sites composing 99.06% of the canopy versus non-drought tolerant species with 0.94%. Total stems counted for drought tolerant species was 8,020 stems versus 159 stems for non-drought tolerant species. Basal area of drought tolerant species was 13,556.34 cm² versus 367.11 cm² for non-drought tolerant species (Table 1.3).

Table 1.3. Diversity, percent cover, stem counts, and basal area metrics for each site surveyed for riparian vegetation. Abbreviations as follows: Mav = Maverick Creek, LaCant = La Cantera, GC1 and GC2 = Government Canyon 1 and 2, respectively.

	Mav	Salado	LaCant	French	GC 1	GC 2	Huesta	Leon
Richness	23	14	8	18	18	15	23	24
Shannon Diversity	2.05	1.68	1.11	1.52	1.99	1.92	1.94	2.18
Shannon Evenness	0.66	0.64	0.54	0.53	0.69	0.71	0.62	0.69
Total Stems	821	1546	607	722	782	1523	1866	312
Total Basal Area (cm²)	2197.3	1651.3	805.3	793.7	1827.6	3368.3	2254.7	1025.4
Percent Cover Drought Tolerant	99.3	100	100	98.9	99.8	99.1	98.6	97

Stems	779	1546	606	714	778	1453	1856	288
Drought								
Tolerant								
Basal Area	2152.8	1651.2	805.1	780	1826.8	3223.4	2179.8	937.2
Drought								
Tolerant								
Percent Cover	99.6	99.4	100	99.4	99	99.9	92.4	98.1
Native								
Stems Native	818	1530	606	711	782	1523	1832	310
Basal Area	2193.1	1633.4	805.1	786.3	1827.6	3368.3	2168.6	1018.9
Native								

The NMDS of canopy cover at the site level had a stress of 0.088 (Figure 1.4), indicating good model fit. There were no strong groupings of site according to percent impervious cover. Leon creek had the most dissimilar community. Government Canyon 2 and French had the most similar communities, although they were different in terms of percent impervious cover. Government Canyon 2 had 0.00% watershed impervious cover, while French had 41.18% watershed impervious cover (Figure 1.4 & Table 1.1). Furthermore, none of the environmental metrics of land use and species traits correlated significantly with site groupings based on the relative abundance of the canopy cover composition.

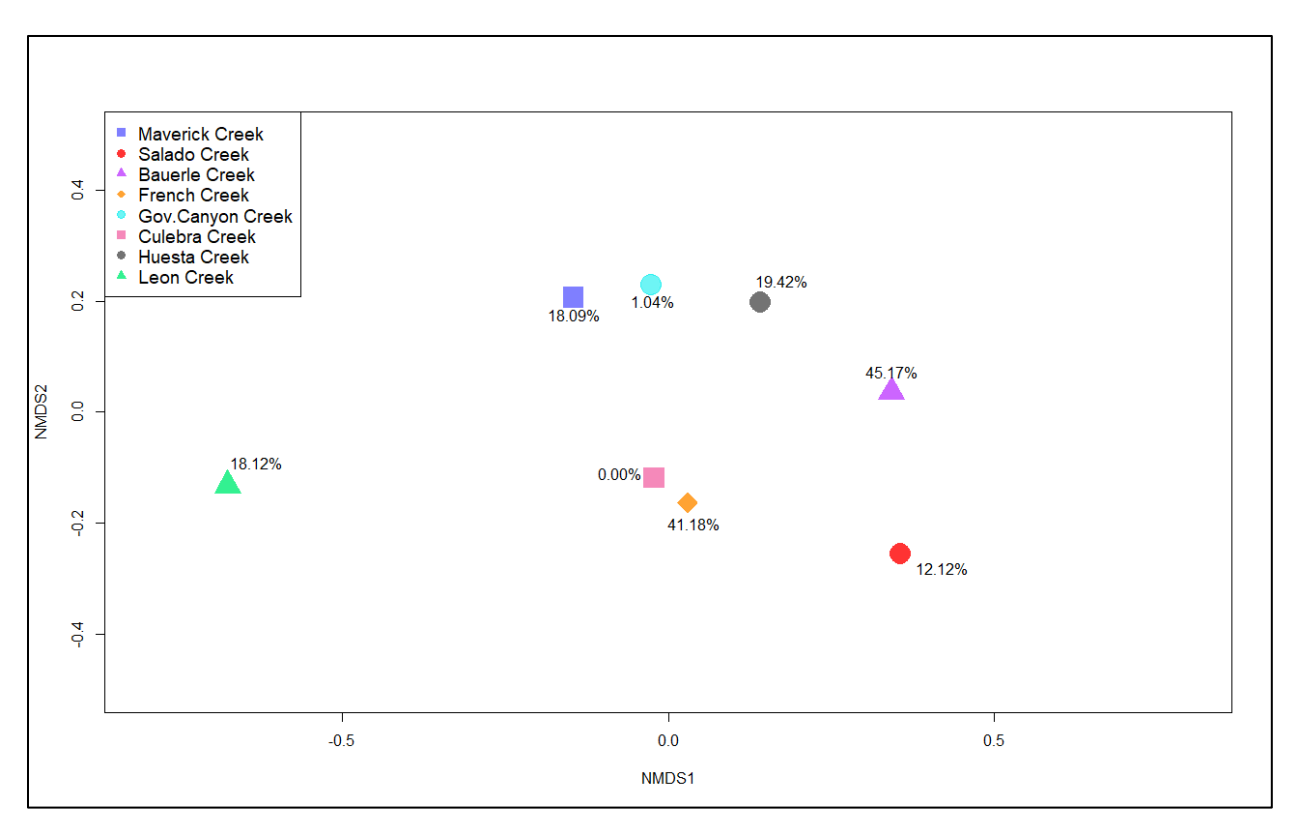


Figure 1.4. Site-level NMDS, showing how sites group together based on relative abundance of woody species as measured by canopy cover.

The NMDS of the basal area had a stress of 0.015 (Figure 1.5), indicating good model fit. Sites were ordered more closely along an urban gradient compared to canopy cover but not perfectly. Multiple land use metrics were found to correlate significantly with site groupings based on basal area. Notably, several indicators of watershed urban development correlated significantly with site groupings: PctUrbLo2019WS (Low Urbanization) (r-square =0.6464, p = 0.081; Figure 1.5), PctUrbMd2019WS (Medium Urbanization) (r-square = 0.6811, p = 0.062; Figure 1.5), PctUrbHi2019WS (High Urbanization) (r-square = 0.6966, p = 0.069; Figure 1.5), and PctImperviuos2019Ws (Impervious Cover) (r-square = 0.7435, p = 0.043; Figure 1.5). These metrics reflect a gradient of community composition along NMDS axis 1 from La Cantera with the highest urban and impervious cover to Government Canyon 2 with the lowest values. PctConif2019WS (Percent conifers) (r-square = 0.8242, p = 0.011; Figure 1.5) represented a contrasting gradient to impervious cover, with highest values at Government Canyon 1 and lowest at La Cantera. Average period between floods (rsquare = 0.82, p = 0.016; Figure 1.5) also correlated with NMDS axis 1, and likely represented a hydrologic gradient from sites with low levels of impervious cover and infrequent floods to sites with high levels of impervious cover and more frequent floods. PctGrs2019Ws (Percent grassland) (r-square = 0.7897, p = 0.028; Figure 1.5) represented a secondary gradient of community composition, with sites with high values of percent grassland, such as Huesta and Leon, separating from sites with lower values of percent grassland.

Several woody species traits were found to correlate significantly with site groupings based on basal area. Both drought tolerance of woody species (r-square = 0.8637, p = 0.014; Figure 1.6) and heat tolerance (r-square = 0.71, p = 0.06; Figure 1.6) were highly correlated with site groupings, and generally aligned with the urbanization gradient along NMDS axis 1. Highest drought tolerance was found at Salado and La Cantera, whereas French was found to have highest heat tolerance. Water use also correlated significantly with site groupings (r-square = 0.7047, p = 0.048; Figure 1.6), but was aligned with NMDS axis 2, with Leon having the highest water use values.

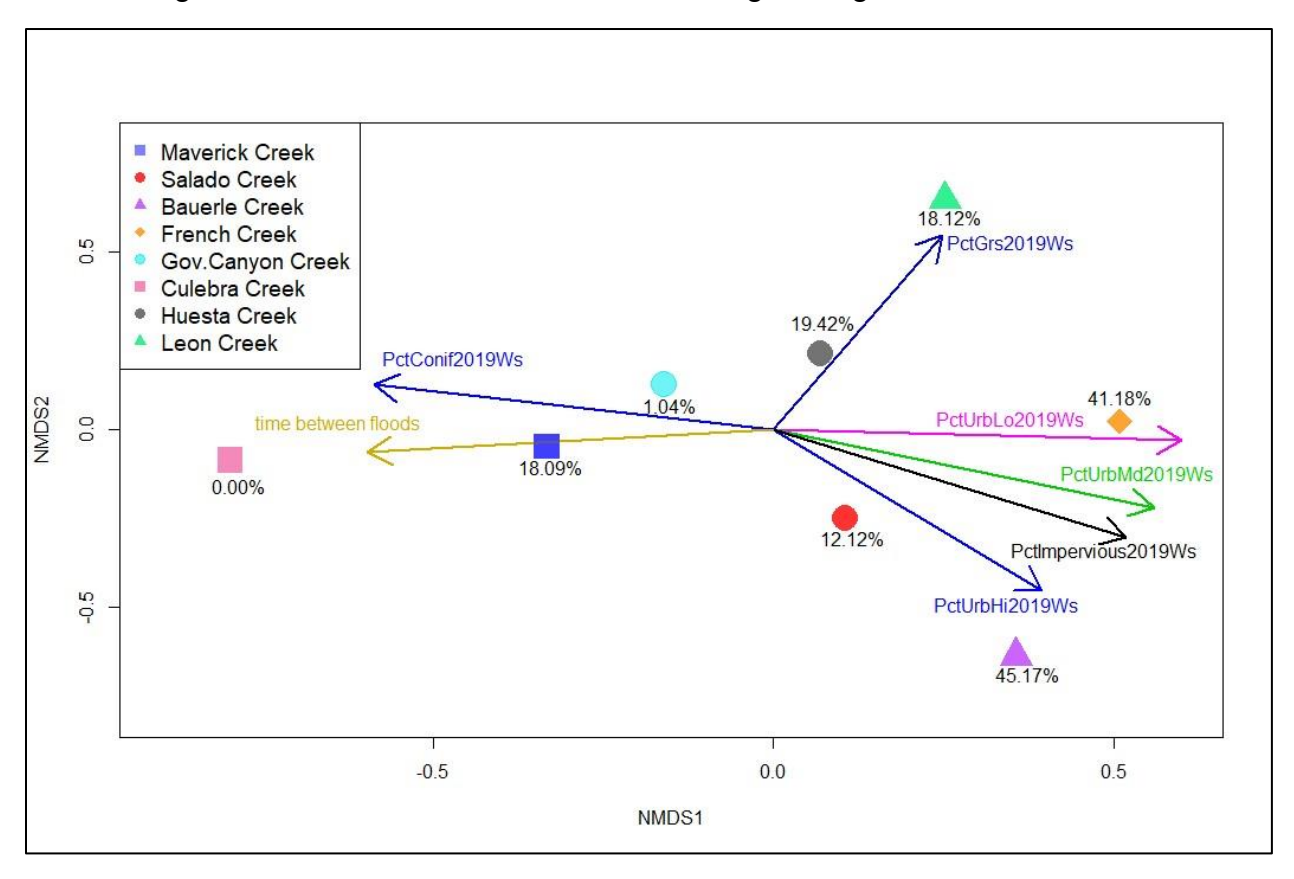


Figure 1.5. Basal area NMDS, with significant land-use and flow metrics plotted as arrows. The length of the arrow is scaled by the strength of the correlation, and weak predictors have shorter lengths than stronger predictors.

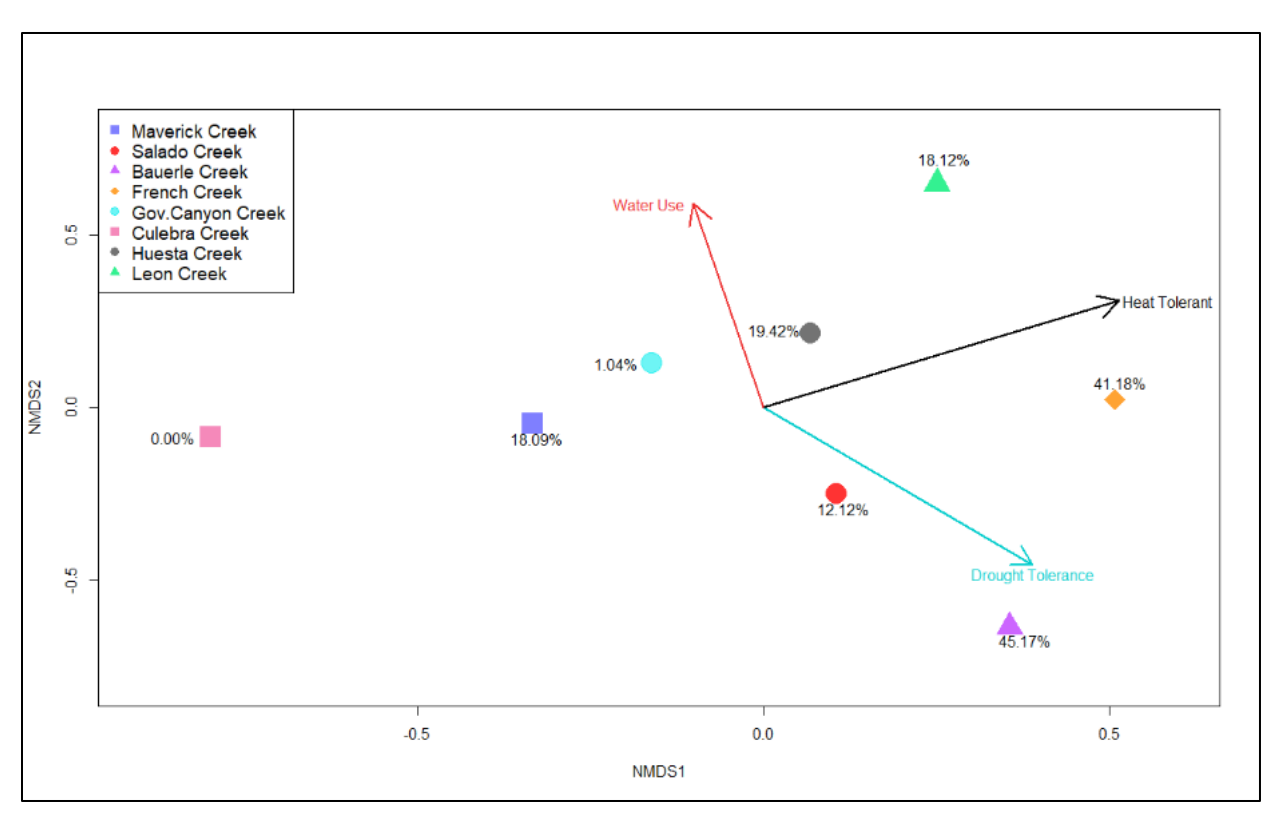


Figure 1.6. Basal area NMDS, with significant woody species traits plotted as arrows. The length of the arrow is scaled by the strength of the correlation, and weak predictors have shorter lengths than stronger predictors.

The NMDS of stem density had a stress of 0.027 (Figure 1.7), indicating good model fit. Sites plotted in a similar pattern to the basal area NMDS and plotted more closely along the urban gradient compared to canopy cover. In regards to environmental fitting metrics, two land use metrics were found to correlate with site groupings based on stem density. PctUrbLo2019Ws (r-squared = 0.627, p = 0.097; Figure 1.7) aligned with a gradient from French creek having the highest levels of low-density urban cover to Government Canyon 2 with lowest levels. Whereas, PctConif2019Ws (r-square = 0.7602, p = 0.022; Figure 1.7) correlated with a gradient from Government Canyon 1 and 2 with highest levels to French Creek with lower levels, indicating Government Canyon 1 and especially Government Canyon 2, are more forested than the rest of surveyed sites. Furthermore, these two locations also face fewer flash flood events than the rest of surveyed sites as they averaged longer periods between floods (r-square = 0.9160, p = 0.002; Figure 1.7). Lastly, drought tolerance (r-squared = 0.7684, p = 0.019; Figure 1.7) was somewhat perpendicular to the land use and flash flood gradient, with Leon having the highest score for drought tolerant woody stems.

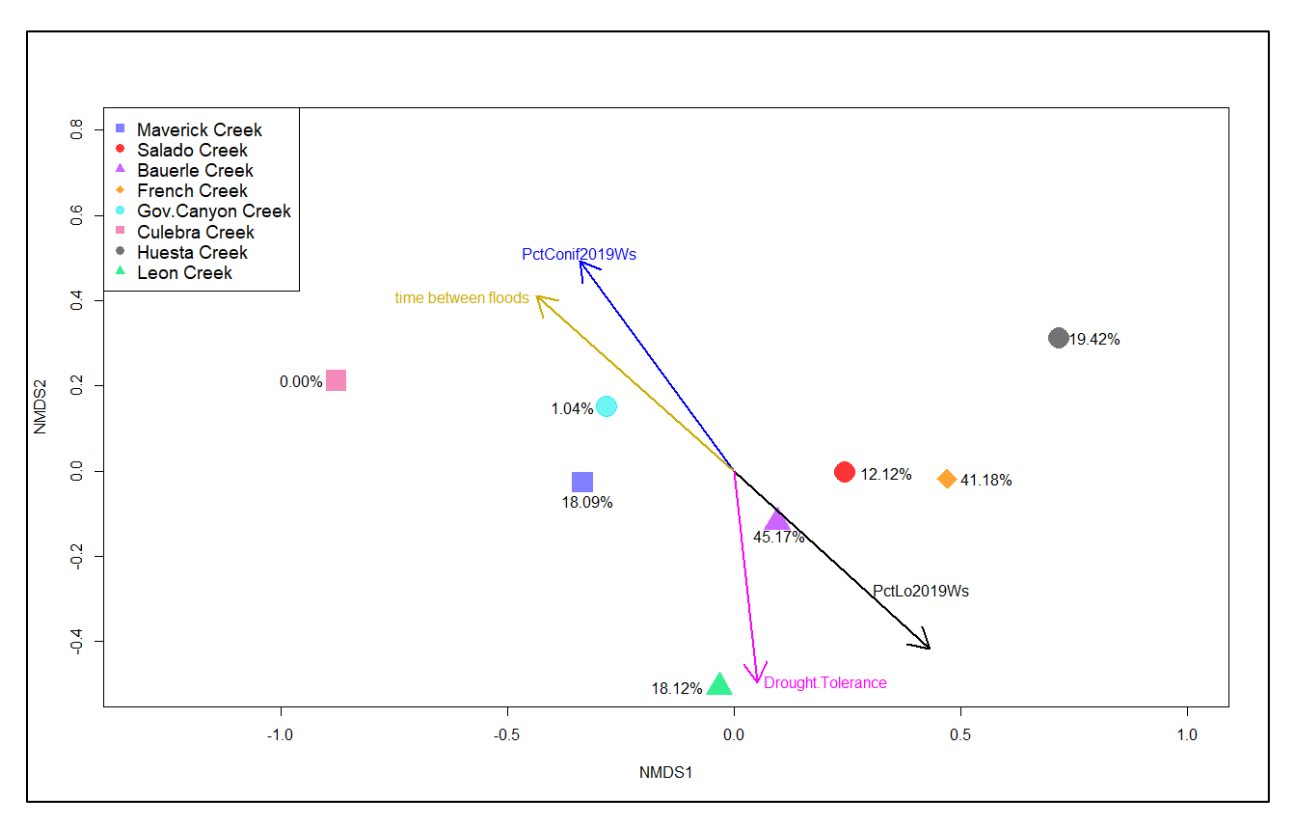


Figure 1.7. Stem density NMDS, with significant land-use and woody species traits plotted as arrows. The length of the arrow is scaled by the strength of correlation, and weak predictors have shorter lengths than stronger predictors.

The NMDS of relative abundance of the canopy cover composition at the geomorphic surface level (Figure 1.8) had a stress of 0.18 indicating adequate model fit. There were no strong groupings of community composition by geomorphic surfaces, indicating that geomorphic surface was not a strong control on community composition as measured by relative abundance of the canopy cover. Instead grouping at the geomorphic surface level was driven by site location. An exception to the grouping of geomorphic surfaces by site location was stream islands (ISL) and secondary active channels (SAC), which were dissimilar to other geomorphic surfaces within site locations. However, neither ISL or SAC surfaces from different sites grouped closely together. Therefore, these geomorphic surfaces stand out as unique within sites, but still dissimilar across sites, at least as measured by relative abundance of the canopy cover composition.

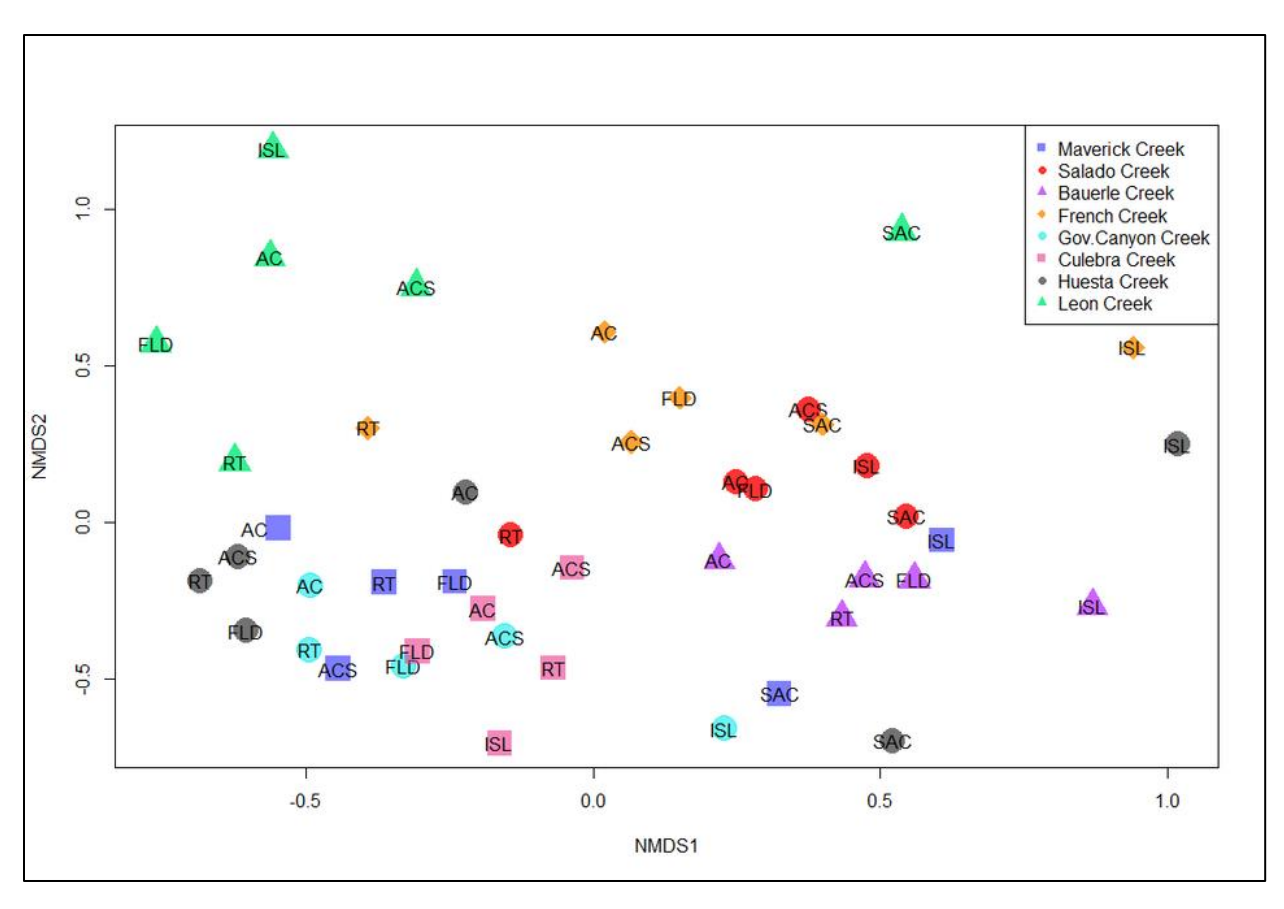


Figure 1.8. Geomorphic surface-level NMDS plot based on relative abundance of canopy cover, with points colored by site type, showing how the geomorphic surfaces group by site. Letters over points identify geomorphic surface type, with AC = active channel, ACS = active channel shelf, FLD = floodplain, RT = riparian terrace, ISL = island, and SAC = secondary active channel

The following variables were found to have a significant negative correlation with impervious cover: average time between floods (r-square of 0.6092, p-value of 0.02227; Figure 1.9), species diversity (r-squared = 0.544, p = 0.03675; Figure 1.10), basal area of medium water use species (r-square of 0.6865, p-value of 0.01104; Figure 1.11), and canopy cover of medium water use species (r-square of 0.4516, p-value of 0.06792; Figure 1.12). One variable was found to have a significant positive correlation with impervious cover: flood events per year (r-square of 0.4972, p-value of 0.05076; Figure 1.13). All other tested relationships were found to be non-significant.

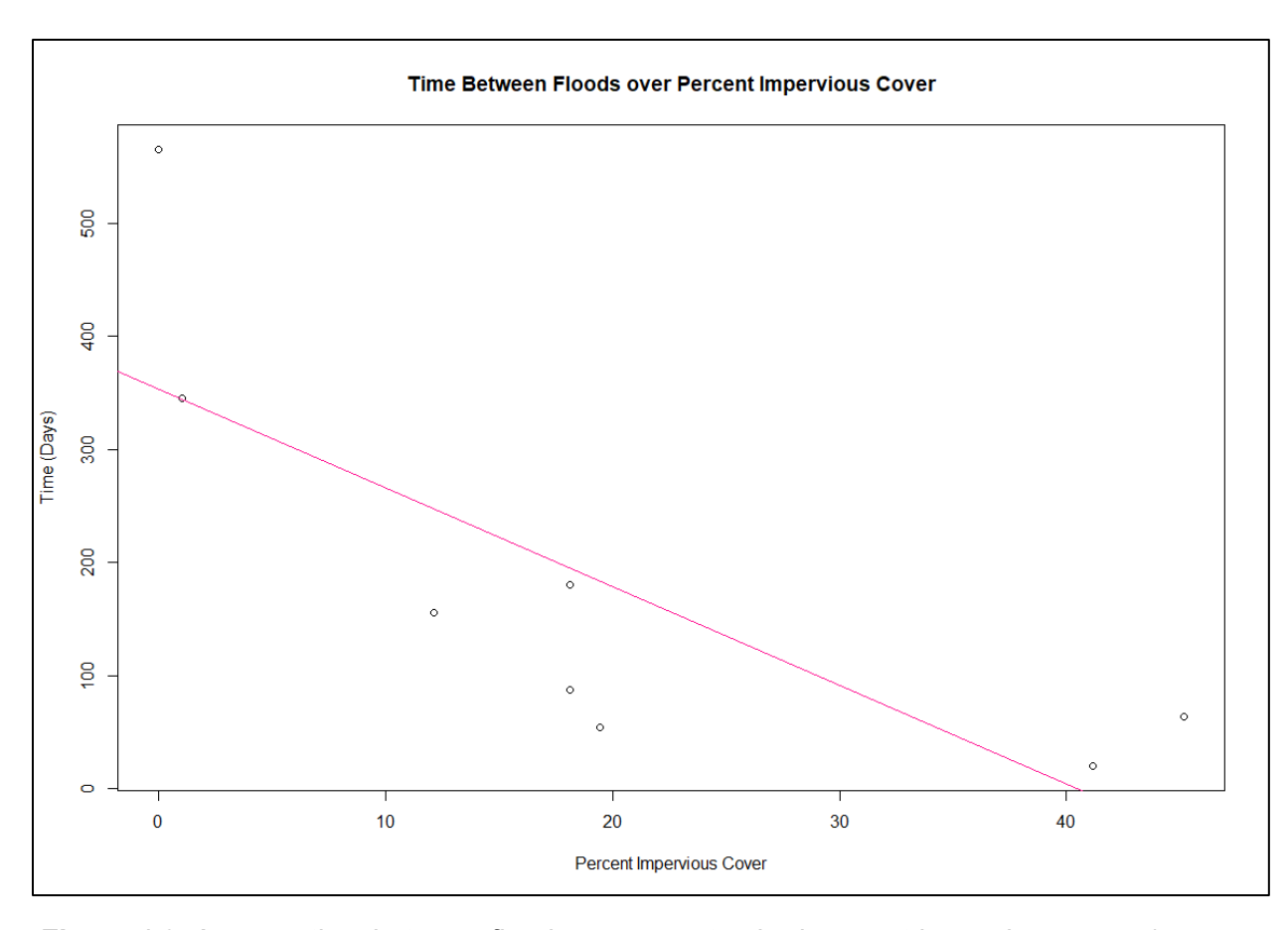


Figure 1.9. Average time between floods versus watershed percent impervious cover (r-square of 0.6092, p-value of 0.02227).

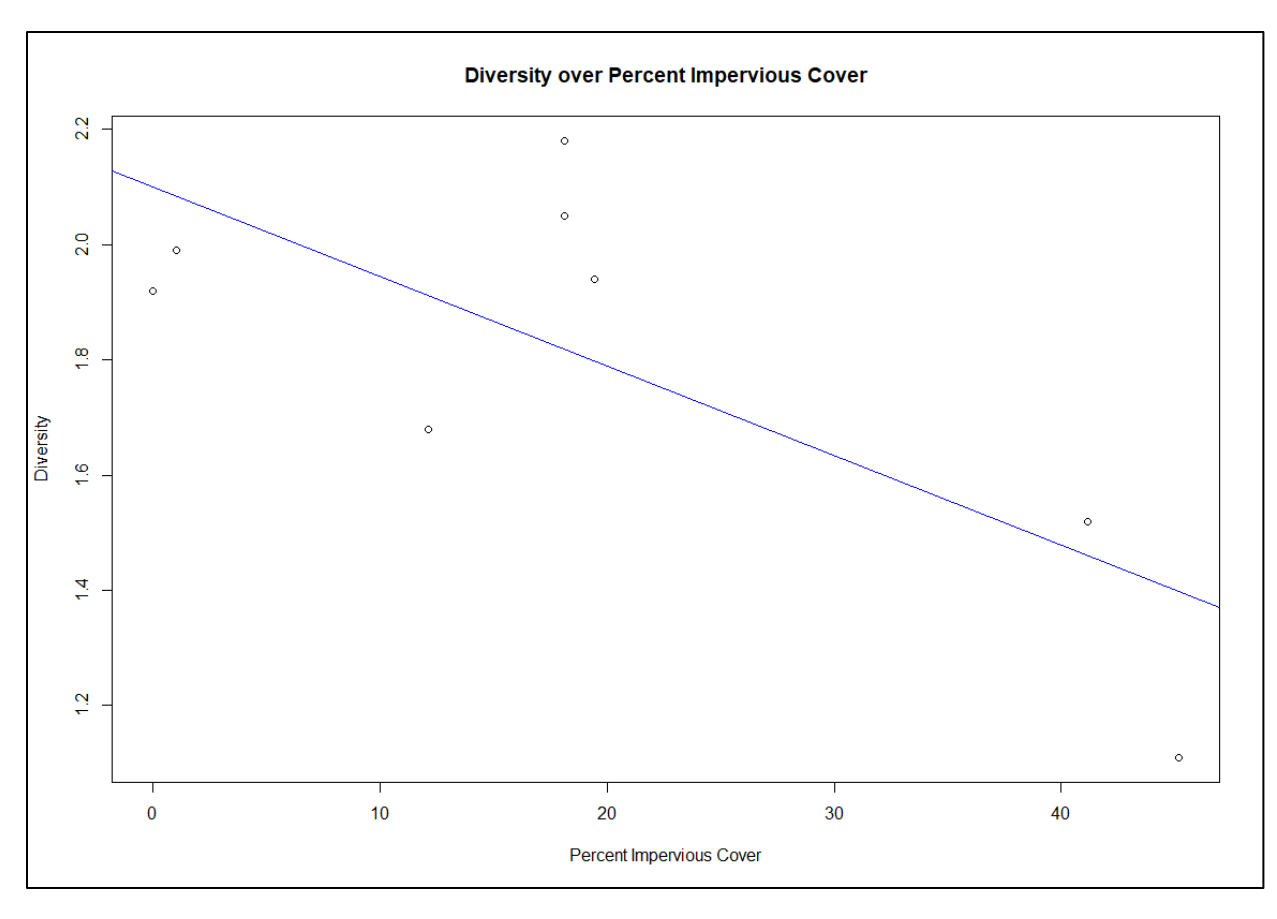


Figure 1.10. Plot of species diversity calculated from canopy cover measurements versus watershed percent impervious cover (r-squared = 0.544, p = 0.03675).

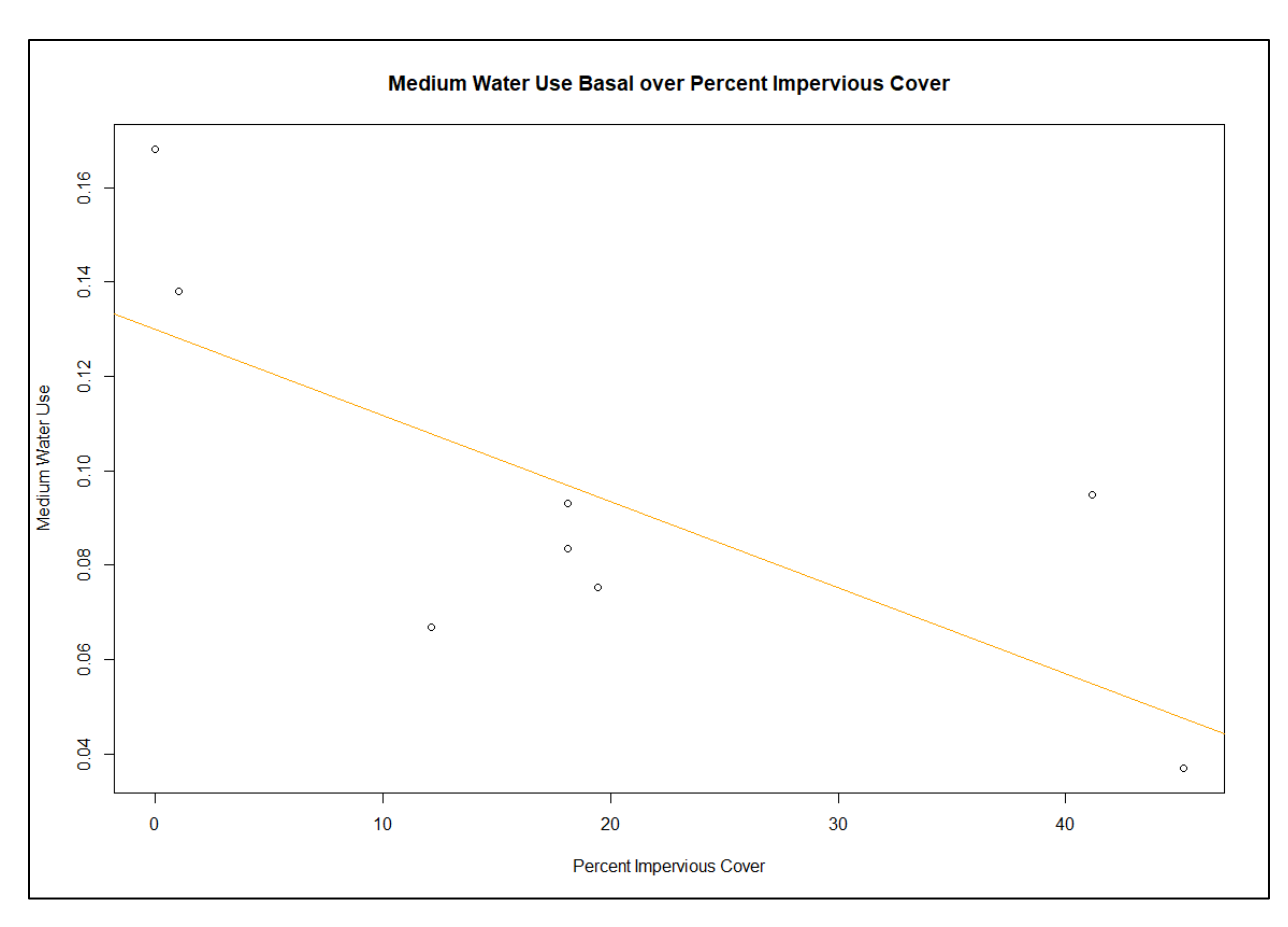


Figure 1.11. Plot of basal area of medium water use species versus watershed percent impervious cover (r-square of 0.5355, p-value of 0.03905).

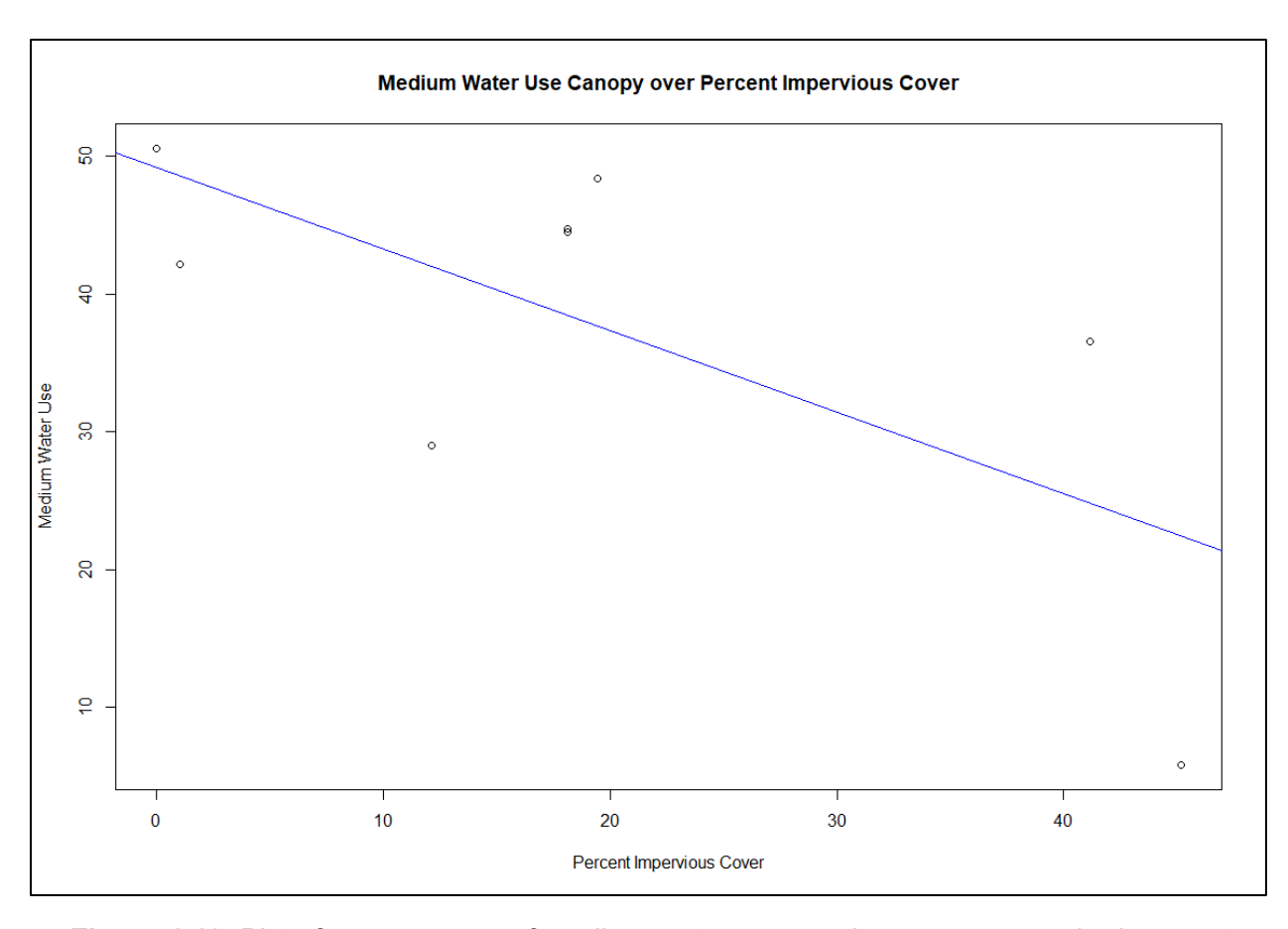


Figure 1.12. Plot of canopy cover of medium water use species versus watershed percent impervious cover (r-square of 0.4516, p-value of 0.06792).

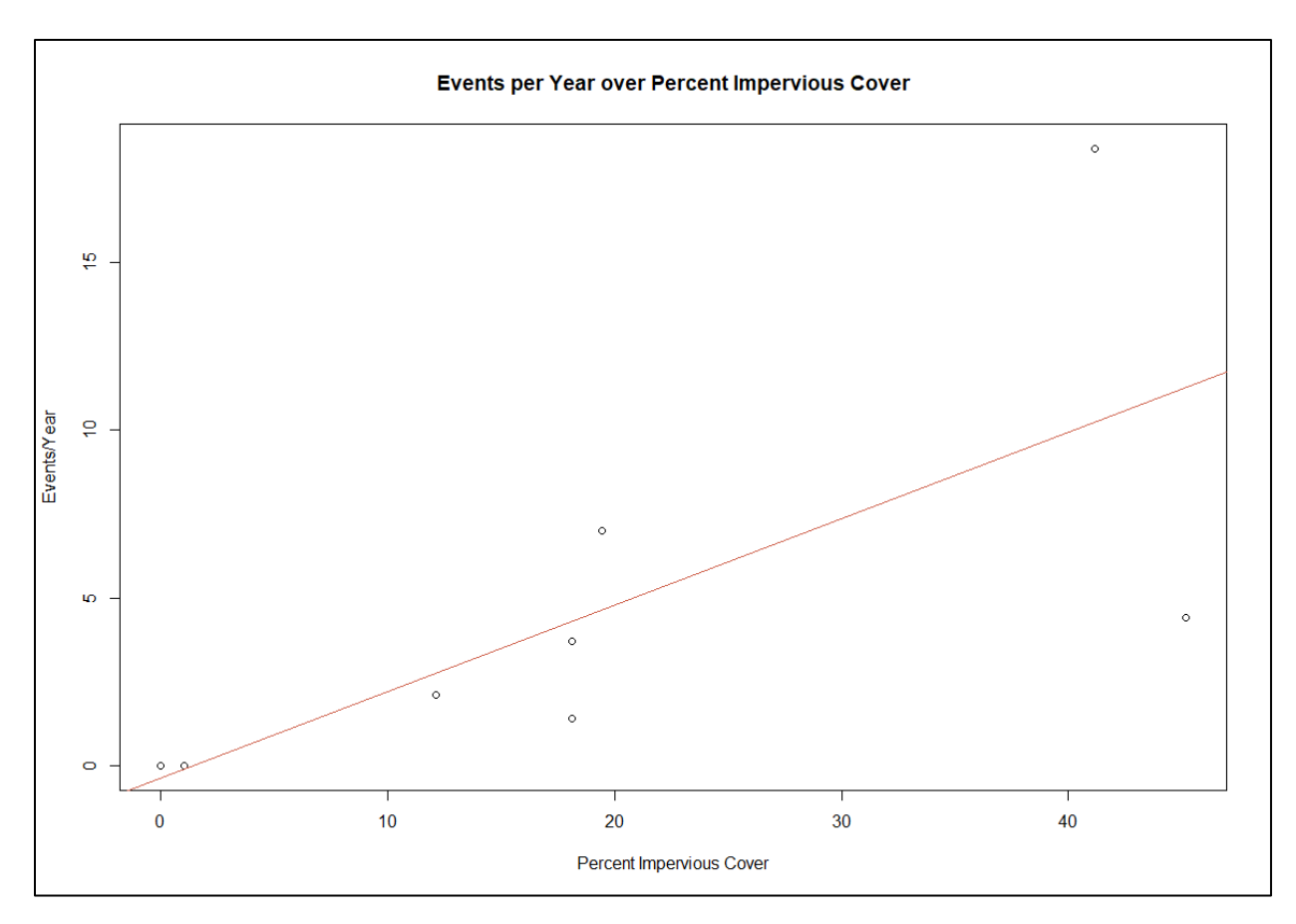


Figure 1.13. Events per year versus watershed percent impervious cover (r-square of 0.4972, p-value of 0.05076).

Discussion

Whether impervious cover did or did not influence hydrology

Whether impervious cover did or did not influence water quality

Riparian vegetation

In order to determine if riparian communities aligned along an urban-to-rural gradient, the community measures of canopy cover, basal area, and stem density were analyzed in relation to land-use and land-cover metrics. Overall results counter the idea that riparian communities group solely based on the amount of impervious cover located in the watershed. Instead, communities grouped based on the combined effects of urban and other land-cover types. Additionally, effects of land use were more evident in the understory of riparian communities, as reflected by basal area and stem density as opposed to canopy cover measurements. The relationship between geomorphic surface elevation and riparian community compositions did not meet our expectations. We saw little influence of elevation on community composition. Finally, we saw that almost all

woody species had some level of drought tolerance, but showed a relationship with land-use on what traits are being selected for.

The conclusion that communities grouped by impervious cover and other land use gradients is shown by the NMDS of stem density (Figure 1.7), and more so basal area (Figure 1.5), which both showed stream sites plotted along an urban-to-rural gradient and secondarily a gradient of grassland cover. An explanation for this plotting pattern may be due to urban patchiness, in that the urban-rural gradient is complicated by other land use types and different spatial arrangements (Pennington, 2010). Urbanization should thus be viewed as a heterogenous disturbance that influences the differences in biotic communities in complex ways, due to the high variation of intensity in urban land cover (Cadenasso et al., 2007 as in Pennington, 2010).

No significant correlations between canopy cover and current land-use metrics were found. A possible explanation for this lack of correlation is the idea of "Temporal Lag" by Pennington (2010), where it is theorized that since the canopy of riparian communities are several decades old and are a climax community, they represent a historical marker and reflect past growing conditions before any urbanization occurred (Pennington, 2010). Likewise, another similar idea is "Land-Use Legacy" by Brice, Pellerin & Poulin (2016), where past land uses such as agricultural practices leave lingering modifications that can still influence community composition for many years.

Analysis from linear regression partially supported the hypothesis that higher levels of impervious cover will lead to lower levels of species richness and diversity. Results showed a negative relationship between impervious cover and diversity as measured by canopy cover (Figure 1.10), but no significant correlation between impervious cover and species richness. The hypothesized mechanism urban development altering riparian communities due to frequent flooding and longer dry periods was also only partially supported. The number of flow events per year had a positive relationship with impervious cover as predicted (Figure 1.13), but average time between floods (days) had a negative relationship with impervious cover (Figure 1.9), contrary to predictions, revealing that sites with higher levels of impervious cover are subjected to more frequent water flow events. The loss of diversity thus can be attributed to urbanization producing infrastructure that diverts and introduces new water flow to riparian ecosystems (Tonkin et al., 2018; Walsh et al., 2005 as in Pennington, 2010). This influx of additional water causes changes to the frequency and length of water flow periods, ultimately altering the overall hydrological pattern and environmental filters (Brice, Pellerin & Poulin, 2016; Solins & Cadenasso, 2019; Poff, 1997). Changing environmental filters can lead to a decrease in diversity if species do not have the appropriate traits to survive increased inundation and are extirpated from a site (Brice, Pellerin & Poulin, 2016; Poff, 1997). The fact that species richness did not significantly correlate with impervious cover suggests species have not been lost overall, but particular species may be increasing in abundance. This result is consistent with other studies, where researchers looking at urban-to-rural gradients have recorded similar

negative correlations as the amount of urbanization increases (Porter et al., 2001; Moffatt et al., 2004; Godefroid & Koedam, 2007 as in Pennington, 2010).

The decline of native species diversity could increase the opportunity for nonnative species to invade local riparian communities (Flanagan, Richardson & Ho, 2015). But contrary to other studies, we did not find any correlation of non-native species with impervious cover, or any influence of non-native species within the community measures. Potential reasons as to why no correlation was found with non-natives are as follows: 1) the distribution of non-native species was patchy and not well sampled by either quadrats or transects, 2) new and emergent urban development, 3) urbanization threshold, and 4) land management and practices. The first reason posits that the distribution pattern of non-native species was not well matched by the sampling approach, as they ranged from a lone individual to large groupings throughout the width and length of survey sites. Furthermore, the placement of transects, and more so quadrats, were randomly determined, such that existing non-native species may have been missed during sampling. According to the second point, the urban development that surrounded the study sites may be recent enough that non-native species have not had the opportunity or time to escape into the surrounding community. Furthermore, when considering the third point, perhaps certain areas in the City of San Antonio have not yet reached an "Urbanization Threshold", meaning that there is still adequate riparian and forested land to negate or offset some of the effects of urbanization. Under this hypothesis, once these lands are cleared and impervious cover is applied, it is expected that this threshold will be surpassed and further alterations to community composition through non-natives could increase. Lastly, perhaps good land management is being practiced and non-natives are being aggressively removed from the community, preventing them from encroaching into the surrounding area.

It was hypothesized that woody species with greater drought and heat tolerance would positively correlate with the percentage of impervious cover, meaning that sites with higher levels of impervious cover would have a greater abundance of drought and heat tolerant species, compared to sites with lower levels of impervious cover, which should have less drought and heat tolerant species. Using linear regression, we tested the following traits: drought tolerance, heat tolerance, and water use, for each of the community measures of canopy cover, basal area, and stem density. Where water use and heat tolerance were furthered subclassified into gradients ranging from low to very high heat tolerance and water use, and drought tolerance only considered species with at least medium levels of tolerance. Results produced a significant negative correlation for the basal area (Figure 1.11) and canopy cover (Figure 1.12) of medium water use species, implying that as the amount of impervious cover increases, the amount of basal area and canopy cover of medium water use species will decline. This finding is consistent with other literature, as Pennington (2010) found that areas with higher levels of impervious cover also had lower levels of medium- and high-moisture woody species, especially in the community measures of canopy cover and stem density. This pattern could be attributed to recent climate behavior as drought and heat conditions are

worsening, creating a hotter and drier environment. This shift may have led to high water-use species to die off, despite frequent flooding. Another explanation for only finding few relationships between impervious cover and drought tolerance was that, the vast majority of sampled species were drought tolerant (99.06%). Lastly, the NMDS and environmental fitting analysis found community measures of canopy cover showed no correlation between any trait tested and impervious cover. This finding is attributed to previously discussed explanation of Temporal Lag and Land-Use Legacy, where the canopy cover is a historical representation of past growing conditions, and therefore the canopy cover may express historical trait values that are not representative of current environmental conditions (Brice, Pellerin & Poulin, 2016; Pennington, 2010). Furthermore, results from the NMDS analysis show that drought and heat tolerance plotted in the same direction of increasing impervious cover, indicating that community measures of stem density (Figure 9), and more so basal area (Figure 7), do support the hypothesis that community measures of heat and drought increased with greater levels of impervious cover. Water use traits plotted towards sites with less impervious cover such as forests and grasslands, further supporting how land use influences and drives variation in riparian community composition (Brice, Pellerin & Poulin, 2016; Tonkin et al., 2018).

A question that arises from these overall results is why medium water use woody species are in decline, even if earlier results indicate there is an overall increase in waterflow? A potential explanation is given by Mitchell (2021), where she describes that higher temperatures accelerate and exacerbate drought conditions, which eventually causes hydraulic failure in woody species. This failure stems from the overall water loss sustained and accumulated during the gas exchange process, and there is no water for the plant to uptake. Under this explanation, woody species are dying off due to tissue death from water loss, resulting from extreme heat, while simultaneously being starved of water due to increasing drought. Urban areas are more likely to have extreme heat, therefore waterflow is not enough to override the hot and dry conditions of urban areas.

In understanding how hydrologic factors such as flooding frequency and geomorphic surface elevation influence community composition, it was hypothesized that surface elevation will significantly affect species composition. More specifically communities found in different geomorphic classifications were predicted to differ from one another. Testing by NMDS signify there was no strong groupings of community compositions by geomorphic surface (Figure 1.8), but communities grouped based on site location instead. This result indicates that riparian communities differ across sites, but communities found on each surface classification within sites are not unique. The expectation was that different surfaces would be flooded at different frequencies, thus driving differences in community composition between surfaces, with more flood-tolerant species on lower surfaces. But the finding was no difference in community composition, suggesting that elevation did not matter. This may be because all floods were large enough to inundate all surfaces or occurred infrequently enough to cause substantial impacts. However, islands, and secondary active channels stood out as the most unique

among all geomorphic surfaces within sites. This result reinforces the earlier discussion on urban patchiness, and that high variation in impervious cover across cities is what influences the differences in community compositions (Alberti et al., 2001 as in Pennington, 2010; Cadenasso et al., 2007 as in Pennington, 2010).

The results have important implications for riparian restoration projects. Identifying historic compositions may in some cases be accomplished by surveying the canopy cover of riparian communities, as it was found in this study that the canopy is a reflection of past growing conditions. Unfortunately, this traditional process does not consider future climatic conditions and land-use, thus rebuilt and restored communities may lack the resilience to survive long-term. An important way to inform restoration in this region would be to extend this study and survey more sites throughout San Antonio, resulting in a large-scale dataset that would allow a better understanding of which creeks are similar to one another, capturing a more accurate and suitable representation of overall riparian community compositions. Such a dataset would allow for a tailored approach to restore and strengthen weakened communities at particular sites, in order to reestablish lost ecosystem functions and services.

Recommendations regarding green infrastructure

Objective 2 – Bioretention Basin Effectiveness

Methods

Site Locations

Three bioretention basins were monitored for Objective 2, along with one natural channel (EC natural) in a mostly forested watershed with a similar watershed size to the bioretention basin drainage areas (Figure 2.1). All bioretention basins were located on the University of Texas at San Antonio main campus (UTSA). Two of the bioretention basins were located on the east side of campus (EC1 and EC2), and treated water draining off a commuter parking lot. The third bioretention basin was built as a demonstration facility for the Mesquite Living Laboratory, located on the west side of campus (see Objective 3), and also treated runoff from a parking lot. The two east campus basins were constructed in xxxx. However, the EC2 basin was improperly constructed initially, and had to be excavated and refilled with biomedia mix in xxxx. The living lab basin was completed in February 2022. The EC1 and living lab bioretention basin were built according to design standards (SARA LID manual), but the EC2 site has excessive silt amounts in the biomedia mix and has a much slower infiltration rate than the other two basins.

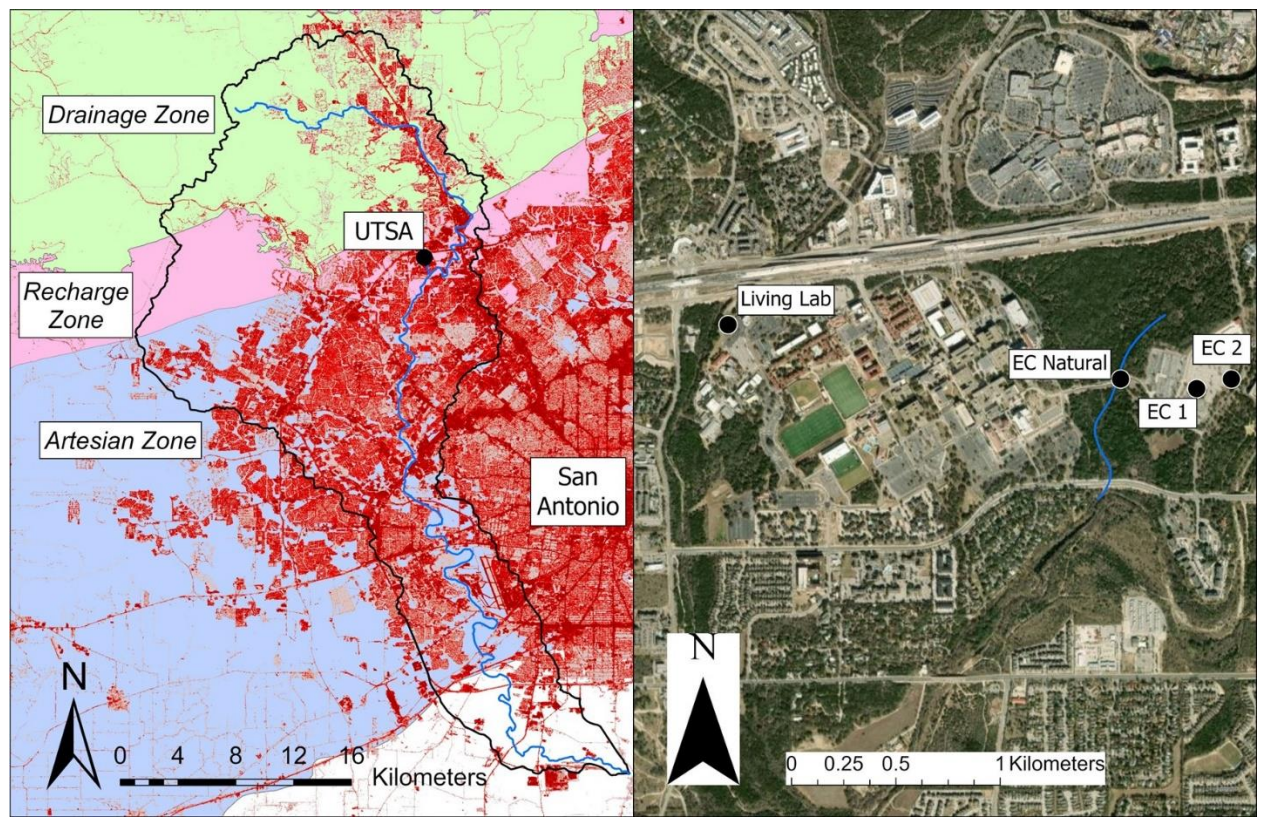


Figure 2.1. Maps showing the location of the UTSA campus relative to San Antonio within the Leon Creek watershed and the Edwards Aquifer Recharge Zone in the left panel, and the location of the living lab bioretention basin, east campus bioretention basins 1 and 2, and east campus natural site in the right panel. Red areas in the left panel show urban developed land.

Flow Monitoring (only includes Living Lab currently)

The water depth during storm events was monitored in the living lab basin and in the outflow pipe of the living lab basin. At all sites, we used bubbler tubing lines attached to flow level loggers (Teledyne Isco Signature flowmeter) to monitor water depth every 5 minutes. In the bioretention basins we attached the bubbler tubing flush with the sediment in the deepest portion of the basin. In the living lab outflow pipe, we affixed the bubbler tubing to the bottom of the outflow pipe, which measured 10.2 cm in diameter.

In the living lab outflow pipe, the water depth was converted to flow rate (Q) by Manning's equation:

$$Q = A \frac{1}{n} R_h^{2/3} S^{1/2}$$

Where A = channel cross-section area, n = Manning's roughness coefficient, R_h = hydraulic radius, and S = slope. A roughness coefficient of 0.01 was used for the outflow PVC piping.

In the living lab basin (inlet sample), the known geometry of the constructed basins was used to convert water depth to water volume. The change in volume of the basins over time during the rising limb of storm events was used to calculate an inflow rate to the basins. The inflow rate to the basins is equivalent to the stormflow that would have occurred in a storm channel if the basins were not present to capture the stormflow (Figure 2.2).

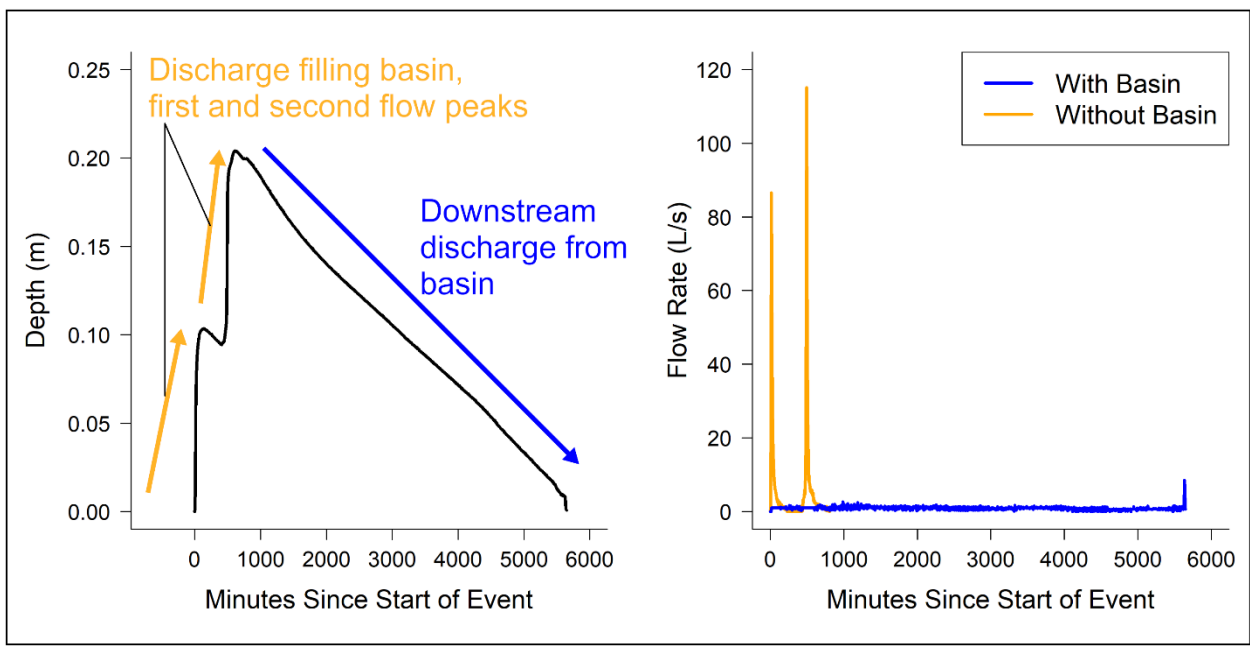


Figure 2.2 (needs to be modified to show just the inflow and for the living lab instead of central campus basin). Example of how the inflow hydrograph to the living lab basin was constructed from changes in water depth over time. The left panel shows recorded changes in depth in the basin during a runoff event. An increase in depth represents inflow to the basin, which would have passed downstream as flow without the basin in place. The right panel shows the resulting flow rate that would have occurred downstream of the basin without the basin in place (orange).

Hydrograph Comparison and Statistical Analysis (only for Living Lab)

To assess the effect of the living lab basin on peak flow levels and flow flashiness, for each flow event recorded, we calculated six metrics from inflow and outflow hydrographs and tested whether flow metrics differed significantly between hydrographs (Table 2.1). We used Shapiro-Wilk tests to check normality assumptions, which informed the selection of parametric versus nonparametric tests. We performed paired Wilcoxon signed rank tests to determine significance of differences between inflow and outflow parameters, since most parameters deviated from normal distributions. We conducted all analyses using the R programming language with the tidyverse (version 2.0.0) and ggplot2 (version 3.4.3) families of packages as well as base R (version 4.3.1) functions (R Core Team 2023).

Table 2.1. Flow metrics calculated from hydrographs.

Metric	Description
Peakflow rate (L/s)	Maximum discharge level during a storm event
Duration (Minutes)	Length of time between start and end of a storm event
Rise time (Minutes)	Length of time between start and peak flow of a storm event
Fall time (Minutes)	Length of time between peak flow and end of a storm event
Average rate of increase (L/s/minute)	Mean slope of rising limb of a storm event
Average rate of decrease (L/s/minute)	Mean slope of declining limb of a storm event

a. Methods Continued

- iv. Water sampling
 - 1. Automatic water samplers Living Lab, EC1 and EC natural
 - **2.** Grab samples for EC2
 - Flow-paced sampling of multiple flushes Living Lab, EC1 and EC natural
 - 4. Water taken back to lab for processing
 - 5. In-situ temperature monitors
- v. Statistical analysis
 - 1. Comparison of input to output for EC1 and EC2 (only event means for EC2, first flushes, event means, loads for EC1)
 - 2. Comparison of effectiveness for event means between EC1 and EC2
 - Comparison of number of events, first flushes, event means, loads for Ec1/2 and and EC natural (only event means for EC2)
 - **4.** Comparison of input to output for Living Lab

Results (living lab hydrology only)

During the monitoring period of 28 June 2022 to 20 April 2023, 30 stormwater runoff events occurred at the living lab basin, of which 19 had matching inflow and outflow data. Two of the events exceeded basin capacity. The inflow hydrograph had significantly higher peak flows, shorter duration, shorter rise times, shorter fall times, and larger average rates of increase and decrease than the outflow hydrographs measured in the outflow pipe (Table 2.2). The median peak flow for the inflow events was 31 L/s and for the outflow events was 6 L/s, representing an 85% reduction. The median total duration of inflow events was 90 minutes, whereas the median total duration of outflow events was 245 minutes (Figure 2.3).

Table 2.2. Table of comparisons between inflow and outflow metrics for the living lab basin with test statistics and p-values.

Metric	Test statistic	p-value	
Peakflow	V = 0	<0.01	
Duration	V = 181	<0.01	
Rise time	V = 177	<0.01	
Fall time	V = 171	<0.01	
Average rate of increase	V = 0	<0.01	
Average rate of decrease	V = 190	<0.01	

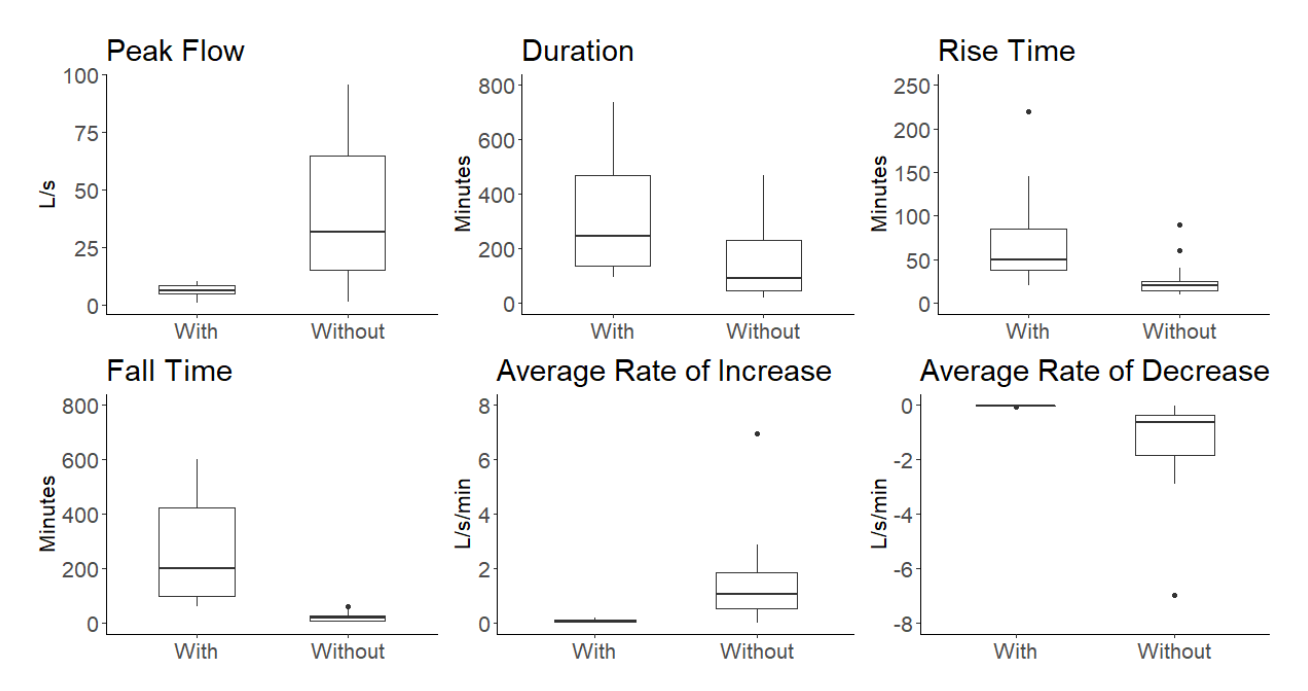


Figure 2.3 (with and without need to be replaced with outflow and inflow). Boxplots showing a comparison of flow metrics between outflow and inflow hydrographs at the living lab bioretention basin.

a. Results continued

- vi. Number of events sampled and dates at each site
- **vii.** Ranges of hydrologic parameters such as number of events and range of peakflows etc.
- viii. Ranges of first flushes, event means, loads at each site
 - ix. Statistical results
 - 1. Input vs output for EC1, 2, and LL
 - 2. Comparison of effectiveness for EC1, EC2 and LL
 - **3.** Comparison of inlet and outlet of basins to EC natural

Discussion (regarding living lab hydrologic impacts only)

The effectiveness of bioretention basins to mitigate flooding issues caused by increasing urban development and recover more natural flow patterns is an important question to address as cities increasingly look to such green stormwater infrastructure investments to manage stormwater runoff. Here, we investigated the impacts of several constructed bioretention basins on downstream flow patterns, including peak flow magnitude and flashiness. Bioretention basins effectively reduced downstream peak flows and flashiness at the small watershed scale (0.055 km²), especially for small to moderate-magnitude flow events, and still attenuated flows effectively even for events that did exceed bioretention basin capacity. Thus, bioretention basins appear to work effectively as stormwater management infrastructure even in environments prone to flash flooding.

The living lab basin significantly reduced peak flow magnitude and metrics of flow flashiness and increased flow duration when comparing incoming hydrographs to outflowing hydrographs. Comparisons of inflowing and outflowing hydrographs from the living lab basin showed the basin decreased peakflows by 83%. Similar magnitudes of peak flow reduction have been found for other bioretention basins (Hunt et al. 2008; Hatt et al. 2009; DeBusk and Wynn 2011; Winston et al. 2016; Lee and Gil 2020), though few other studies have investigated impacts to flow flashiness (Hood et al. 2007; Damodaram et al. 2010; Li et al. 2017). Increase in flashiness caused by urban development, combined with higher peak flood magnitude, often leads to downstream channel erosion and incision (Walsh et al. 2005). Thus, the mitigation of urban-driven increases to flow flashiness by the bioretention basins should help prevent degradation of channel habitat in watersheds undergoing development.

The reduction in peak flow volume and flow flashiness and increase in flow duration is due to the capturing of runoff by the basins during storm events, followed by a slow release of the stored water over a longer time as the water infiltrates through the basin soil and into the underdrain. The capacity of the living lab basin was only exceeded by two events. Flow events with a larger total volume would have filled up the basins and bypassed the basins through overflow piping. Such flow events thus were likely less effectively attenuated, though the filling of the basins still reduced peak flow rates and flashiness downstream to some degree. Other

studies have similarly found a higher effectiveness of retention basins for small to moderate flood events (Hoss et al. 2016; Juan et al. 2016; Sun et al. 2019; Wang et al. 2019).

The effectiveness of the basins in attenuating peak flows and reducing flashiness shows that new urban developments can be effectively treated to reduce peak flows in local channels with bioretention basins. The living lab basin had a small area relative to the watershed area treated, showing that treatment of stormwater from new developments can occur with relatively little land area devoted to green stormwater infrastructure (Guerrero et al. 2020). Beyond land requirements, constructability is a key factor in determining the applicability of green stormwater infrastructure to treat any new development project or retrofit existing untreated development. Proper construction of bioretention basins, such as installation of biomedia to design specifications, influences long term maintenance and operation and long-term performance (Nazarpour et al. 2023). Such constraints will need to be considered when evaluating the cost effectiveness of green stormwater infrastructure in any particular location (Houle et al. 2013; Zeng et al. 2020).

The bioretention basins studied here were constructed in a region with a climate typical of many arid or semi-arid and tropical climates, which often experience long periods without precipitation punctuated by high-intensity rainfall and runoff events. High-intensity and largemagnitude events can overwhelm basin capacity, but long antecedent dry periods between runoff events could be beneficial, allowing time for evaporation to increase storage capacity and water retention (Mahmoud et al. 2019). On the other hand, prior research has often found bioretention basins and other green stormwater infrastructure less effective during large magnitude and high-intensity events (Holman-Dodds et al. 2003; Damodaram et al. 2010; Tao et al. 2017). Our flow monitoring in a hydrologically variable climate showed that bioretention basins are effective at mitigating hydrologic impacts of urban development locally, and even though large events can overwhelm storage capacity, peak flows and flow flashiness are still reduced compared to the untreated condition. Further research into the water quality effectiveness of green stormwater infrastructure in similar environments is warranted since water quality treatment effectiveness depends on soil saturation conditions and resulting redox potentials within basins (Dietz and Clausen 2006; Mangangka et al. 2015; Alam et al. 2021). Water quality treatment effectiveness may also be compromised by long dry periods due to loss of vegetation unless irrigation is supplied (Lizárraga-Mendiola et al. 2017; Barron et al. 2020), although appropriate design guidance may alleviate this issue (Houdeshel et al. 2012). Regardless of water quality impacts, combined with the potential additional benefits of bioretention basins, especially when integrated into land use planning (Yang and Li 2013), such as water quality treatment (Li and Davis 2009; Trowsdale and Simcock 2011; Kim et al. 2012; Johnson and Hunt 2019), downstream channel physical habitat protection (Anim et al. 2019), wildlife habitat (Loperfido et al. 2014), groundwater recharge (Alamdari and Hogue 2022b), promoting resilience to climate change (Pyke et al. 2011), and green space in urban areas, which can provide cooling, recreational, education, and aesthetic benefits (Tzoulas et al. 2007; Prudencio and Null 2018; Liu et al. 2021), green stormwater infrastructure projects are likely to be cost-effective methods for managing stormwater runoff from new developments, even in areas prone to flash flooding.

b. Discussion continued

- x. Effectiveness of basins in to out and versus natural system
- **xi.** Reasons for any differences between basins (infiltration rates could be useful here)
- **xii.** Any recommendations for future basin installation

Objective 3 – Community Education

Education of K-12 students, college students, and water management professionals about the Edwards Aquifer and threats to the aquifer is an important component of protecting and managing the Aquifer sustainably for future generations. Toward this end, the project included the building of a living laboratory with demonstration green stormwater infrastructure facilities and a commitment from UTSA to use the facility for water resource education. The facility construction and education activities comprise Objective 3 of the overall project.

Mesquite Living Lab and LID Features

Construction of a building and associated demonstration green stormwater infrastructure facilities, which was later named the Mesquite Learning Lab, began in November 2020 and was completed by February 2022 (Figure 3.1). The building is located on the west side of the University of Texas at San Antonio main campus and backs up onto Maverick Creek, an ephemeral stream channel which was sampled as part of Objective 1 of this project. The building is composed of three sections with a total indoor space of approximately 2,000 square feet. The largest section is a screened-in, open-air classroom with movable tables, chairs, and audio-visual equipment (Figure 3.2). A wraparound porch on two sides of the open-air classroom provides overlooks of the bioretention basin feature that was included during construction of the building (Figure 3.3). The other two building sections are a restroom facility (Figure 3.4) and several offices with an adjoining storage closet (Figure 3.5), which are air-conditioned. The building is ADA accessible (Figure 3.6) and includes an outdoor gathering area in back of the building (Figure 3.7), which includes repurposed pink granite seats. Repurposed pink granite was also included in the main building façade (Figure 3.1). The shape of the rooftop of the building resembles a butterfly when viewed directly from above (Figure 3.8).

Three demonstration low impact design features were incorporated into the Living Lab footprint. The first is a cistern with a capacity of xxxx gallons, which captures water from the rooftop over the classroom and offices (Figure 3.9). The cistern helps mitigate the contribution of the building footprint to downstream flood peaks by capturing water draining off the roof during rain events. The captured water is released after the rain event has ended, such that the captured water does not contribute to runoff during the time when peak flood levels occur during a storm. The second LID feature is a

green roof over the restroom facility (Figure 3.10). The green roof helps reduce runoff from the footprint of the restroom facility by allowing soil and vegetation to capture some water during rain events. The green roof also helps reduce cooling costs for the restroom facility by providing natural insulation and shade for the building.

The third LID feature is a bioretention basin (Figure 3.1). The bioretention basin captures runoff from approximately one acre of parking lot surface. Water that drains into the bioretention basin is ponded temporarily and then filters through a soil biomedia mix with a depth of at least two feet. After water filters through the biomedia mix, it is captured by a perforated PVC underdrain and conveyed by gravity to an outlet drain, which feeds into a larger, previously constructed stormwater sand filter basin near the Living Lab. The basin was constructed according to standards detailed in the SARA LID manual (Lid Manual citation). The basin is lined with an impermeable liner. A layer of #51 gravel was placed atop the liner and around the perforated PVC underdrain. A four-inch layer of soil media barrier composed of washed sand and ASTM-8 choker stone was placed between the gravel and the biomedia mix. A layer of cobbles was placed atop the biomedia mix. The bioretention basin also helps reduce downstream peak flood levels through a similar mechanism as the cistern, as demonstrated in Objective 2. The bioretention basin also helps remove pollutants from stormwater running off the parking lot, as demonstrated in Objective 2.

Maintenance Plan for Mesquite Learning Lab LID Features

Maintenance of the LID features involves managing vegetation, periodically checking the proper infiltration of the bioretention basin, and performing clean-out or other maintenance tasks when problems are identified. Vegetation in the bioretention basin is cut with hand trimmers approximately twice a year and cut vegetation is removed from the basin to prevent reductions in infiltration rates. The green roof is watered once a week to ensure vegetation persists through periods between rainfall events. The cistern is opened after rainfall events and the "first flush" pipe is checked and drained periodically to ensure proper function.

Infiltration in the bioretention basin is monitored opportunistically after rainfall events to ensure surface water does not persist in the basin for longer than 72 hours. To date, no issues have been identified with infiltration, but flushing of underdrains using clean-out pipes or replacement of the top few inches of biomedia mix may eventually be required if infiltration rate ever becomes too low.



Figure 3.1. Photograph of the Mesquite Living Laboratory, showing the curb cuts that allow parking lot runoff to flow into the bioretention basin in front of the building and the repurposed pink granite forming the building façade. The sycamore tree in the foreground is planted in a tree box within the bioretention basin. The other trees in the picture are live oaks and were preserved through construction of the building. Plants on the green roof are also visible just above the building sign.



Figure 3.2. Photograph of the open-air classroom space at the Mesquite Living Laboratory.



Figure 3.3. Photograph of summer camp students on the wraparound porch in front of the open-air classroom at the Mesquite Living Laboratory. Cobbles in foreground mark the bioretention basin. Photo Credit: J. Chavez.



Figure 3.4. Photograph of the restroom facilities at the Mesquite Living Laboratory.

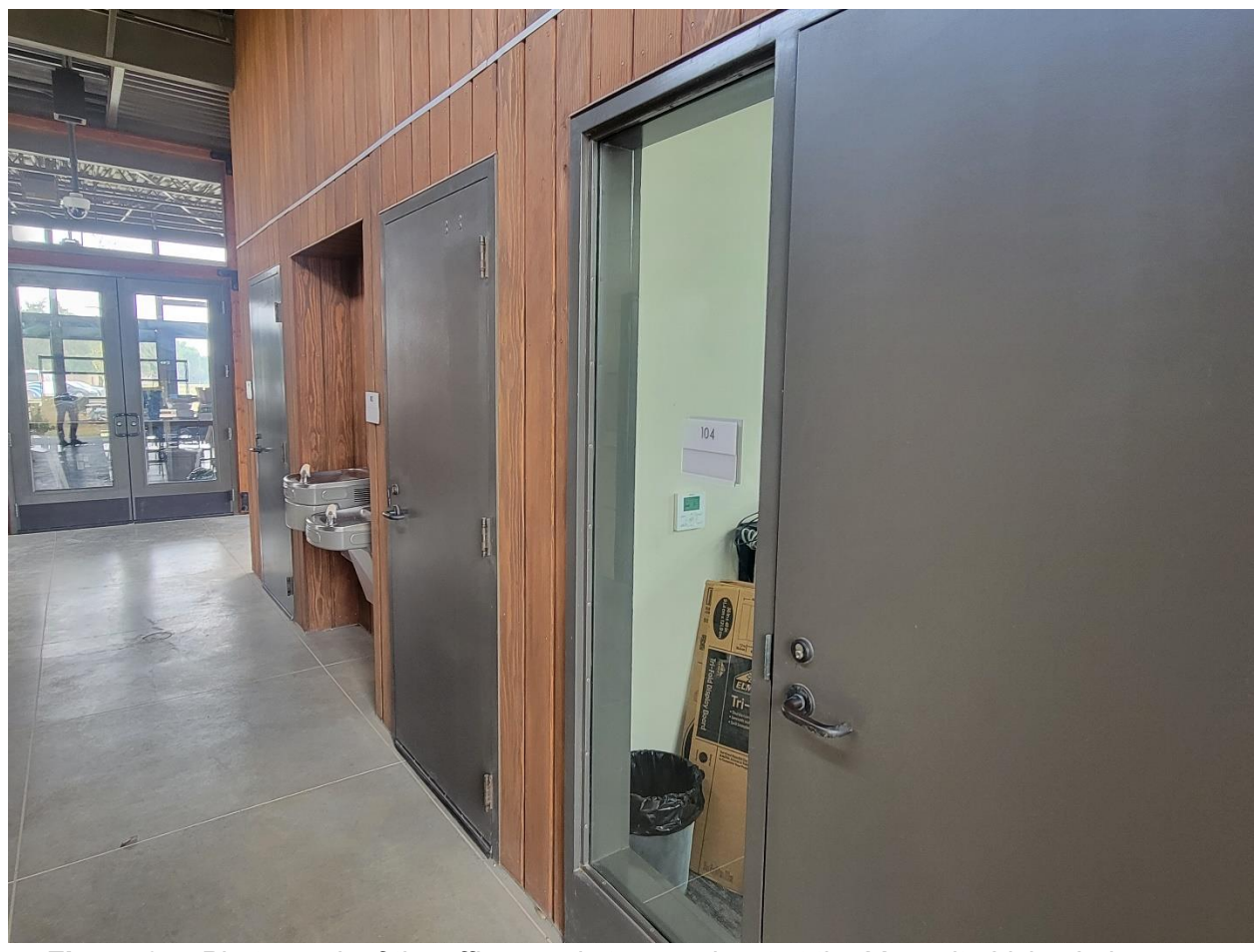


Figure 3.5. Photograph of the offices and storage closet at the Mesquite Living Laboratory.



Figure 3.6. Photograph of the ADA parking spaces and access at the Mesquite Living Laboratory.



Figure 3.7. Photograph of the outdoor amphitheater with repurposed pink granite benches at the Mesquite Living Laboratory.



Figure 3.8. Aerial view of the Mesquite Living Laboratory, showing the approximate surface area of one acre, outlined in black, that drains to the bioretention basin. The blue line on the left of the picture shows the location of Maverick Creek. Also visible in the top of the picture is the existing sand filter basin which receives water from the underdrain of the bioretention basin.



Figure 3.9. Photograph of the cistern at the Mesquite Living Laboratory.



Figure 3.10. Photograph of the green roof atop the restroom facility at the Mesquite Living Laboratory.

Education and Outreach Activities at the Mesquite Living Laboratory

Since construction finished in early 2022, multiple education and outreach events have been hosted at the Mesquite Living Laboratory (Table 3.1). The primary educational program occurring at the lab is a summer camp, which has been held each year at the lab, starting in 2022. The summer camp is a four-week block of individual one-week sessions, with the first two weeks focused on pollinators and the second two weeks focused on hydrology (Figure 3.11), but hydrological topics are discussed during the pollinator camps. Two campus visits by the EWRI have been hosted at the lab, and included tours of the lab and green stormwater infrastructure facilities. Several other activities have also been hosted at the lab.

Official surveys of student learning are planned for implementation at summer camps this year (2024). However, several informal lines of evidence suggest the summer camp programs are benefitting students. Several parents and teachers of

students who have attended the pollinator camps have provided feedback that the students did well on certain components of standardized tests during the subsequent school year, including the life cycle of insects. Other parents have shared that some students expressed more interest in pursuing science careers and interests after attending the camps.

Students at UTSA have benefitted from the building and associated education and research as well. The summer camps benefit current UTSA undergraduate and graduate students who help with the camps, as they gain experience in public education and outreach. Students have been able to attend multiple events held at the laboratory (Table 3.1). In addition, approximately ten undergraduate students have been directly involved with research at the living lab, either as volunteers during field and laboratory work, or more directly through independent study projects. The experience with scientific research is an important opportunity for students beyond the classroom education.

Table 3.1. Information on education and outreach activities that have been hosted at the Mesquite Living Laboratory since construction completed in early 2022.

Event Title	Description	Participants	Dates Held	Number of Participants
Summer camps	Four individual one-week, all day camps where participants learn environmental science topics including pollinators and hydrology	6-12 year olds	Summer 2022, 2023, planned for 2024	240 (120 each summer)
EWRI Tour	Tour of UTSA stormwater management facilities for the San Antonio Chapter of the Environmental & Water Resources Institute (EWRI, including the Mesquite Living Lab and associated green stormwater facilities.	Water management professionals and some UTSA students	Spring 2023 and 2024	60 (30 each tour)
San Antonio CAB Meeting	Monthly meeting of the Conservation Advisory Board (CAB), which included presentation of preliminary results about effectiveness of Mesquite Living Lab green stormwater facilities	Advisory board members, other professionals, some UTSA students	Nov. 3, 2023	30
USFWS BBQ	Afternoon BBQ designed to facilitate networking between visiting	USFWS professionals, UTSA	October 2022, March	200 (50 each event)

Fish and Wildlife Service	students and faculty	November	
(USFWS) and UTSA		2023, April	
faculty and students		2024	



Figure 3.11. Photograph of students forming a meandering river channel during the hydrology summer camp. Photo Credit: J. Chavez

Discussion

Construction of the Mesquite Living Laboratory and associated green stormwater infrastructure facilities, including a cistern, green roof, and bioretention basin, was completed in early 2022. Since construction was completed, multiple educational activities have been held at the laboratory for grade school children, UTSA students, and water management professionals. In summer 2022 and 2023, approximately 120 students, aged 6-12, attended camps to learn about hydrology and other environmental science topics. Another 120 students will attend camp in summer 2024. Undergraduate and graduate students at UTSA have interacted with professionals in the environmental science field and several have been directly involved with research at the lab. Water management professionals have toured the green stormwater infrastructure facilities to learn how they work and how they are performing. Thus, the lab is being used for education and outreach purposes as intended.

Personnel at UTSA plan to continue current educational activities at the Mesquite Living Laboratory and develop additional activities. The summer camps are being held this year (2024), and will continue in future summers. Discussions are underway with the San Antonio River Authority (SARA) to fund day trips of school groups to the living lab for water-resource education activities. Such trips would occur during the school year and would ideally service schools throughout the city. Another activity planned in the future for the living lab is to host high-school students who are taking dual-credit courses at South Texas College in the Rio Grande valley. Personnel are also developing grant proposals to different federal agencies that could fund development of educational materials, such as an outdoor stream lab or large murals of the Edwards Aquifer and contributing and recharge zones and hydrological processes.